Accepted Manuscript

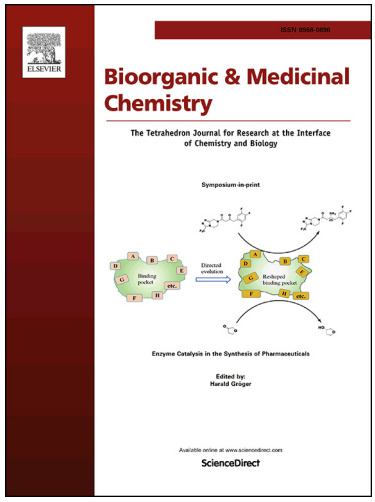

Synthesis and Biological Evaluation of Irreversible EGFR Tyrosine Kinase Inhibitors Containing Pyrido[3,4-*d*]pyrimidine Scaffold

Hao Zhang, Jin Wang, Hong-Yi Zhao, Xue-Yan Yang, Hao Lei, Minhang Xin, Yong-Xiao Cao, San-Qi Zhang

PII: S0968-0896(18)30793-4
DOI: https://doi.org/10.1016/j.bmc.2018.05.039
Reference: BMC 14381

To appear in: *Bioorganic & Medicinal Chemistry*

Received Date: 24 April 2018
Revised Date: 21 May 2018
Accepted Date: 23 May 2018

Please cite this article as: Zhang, H., Wang, J., Zhao, H-Y., Yang, X-Y., Lei, H., Xin, M., Cao, Y-X., Zhang, S-Q., Synthesis and Biological Evaluation of Irreversible EGFR Tyrosine Kinase Inhibitors Containing Pyrido[3,4-*d*]pyrimidine Scaffold, *Bioorganic & Medicinal Chemistry* (2018), doi: https://doi.org/10.1016/j.bmc.2018.05.039

Synthesis and Biological Evaluation of Irreversible EGFR Tyrosine Kinase Inhibitors Containing Pyrido[3,4-*d*]pyrimidine Scaffold

Hao Zhang [a], Jin Wang [b], Hong-Yi Zhao [a], Xue-Yan Yang[a], Hao Lei [a], Minhang Xin [a], Yong-Xiao Cao [b], San-Qi Zhang [a *]

[a] Department of Medicinal Chemistry, School of Pharmacy, Xi′an Jiaotong University, Xi′an, Shaanxi, 710061, PR China

[b] Department of Pharmacology, School of Basic Medical Science, Xi′an Jiaotong University, Xi′an, Shaanxi, 710061, PR China

[*]Corresponding author: sqzhang@mail.xjtu.edu.cn (S. Q. Zhang).

Abstract

In the present study, a new class of compounds containing pyrido[3,4-*d*]pyrimidine scaffold with an acrylamide moiety was designed as irreversible EGFR-TKIs to overcome acquired EGFR-T790M resistance. The most promising compound **25h** inhibited HCC827 and H1975 cells growth with the IC_{50} values of 0.025 μM and 0.49 μM, respectively. Meanwhile, **25h** displayed potent inhibitory activity against the $EGFR^{L858R}$ (IC_{50} = 1.7 nM) and $EGFR^{L858R/T790M}$ (IC_{50} = 23.3 nM). **25h** could suppress EGFR phosphorylation in HCC827 and H1975 cell lines and significantly induce the apoptosis of HCC827 cells. Additionally, compound **25h** could remarkably inhibit cancer growth in established HCC827 xenograft mouse model at 50 mg/kg *in vivo*. These results indicated that the 2,4-disubstituted 6-(5-substituted pyridin-2-amino)pyrido[3,4-*d*]pyrimidine derivatives can serve as effective EGFR inhibitors and potent anticancer agents.

Keywords

pyrido[3,4-*d*]pyrimidine; EGFR-TKIs; anticancer; irreversible inhibitors; drug design

1. Introduction

Receptor tyrosine kinases (RTKs) play an important role in the regulation of cell growth, survival, and differentiation.[1] Constitutive activation and/or over-expression have been observed in numerous human tumors such as breast, ovarian, colon and non-small cell lung cancers (NSCLC). Epidermal growth factor receptor (EGFR) is among the known RTKs and has been extensively studied. As a number of the families of ErbB, EGFR tyrosine kinase has been validated as one of the most effective targets for the treatment of NSCLC.[2, 3] So far, there are thousands of EGFR tyrosine kinase inhibitors (EGFR-TKIs) were synthesized and evaluated. For NSCLC patients harboring activating mutations (e.g., L858R and exon 19 deletion), the first-generation EGFR-TKIs gefitinib and erlotinib (Fig. 1) showed effective tumor regressions and improved progression-free survival (PFS).[4-6] However, after about one year of treatment, these anti-tumor effects are counteracted owing to drug-resistance caused by T790M mutation.[7] The transformation of threonine toward bulkier methionine not only provokes a significant steric repulsion with the 4-aminoquinazoline-based inhibitors but also increases the affinity of EGFR to ATP, rendering first-generation ATP-competitive inhibitors less effective.[8, 9] To overcome the resistance, the modification of the 6-substituted group in 4-anilinoquinazolines with the group bearing active group provided the inhibitors with improved potency.[10-13] Likewise, the replacement of 6-substituted group in gefitinib with acrylamide moiety produced the second-generation irreversible EGFR inhibitors including afatinib[14] (Fig. 1), dacomitinib[15] and neratinib[16]. Afatinib demonstrated high activity against T790M mutation and approved by FDA in 2013. Nevertheless, afatinib failed to distinctly improved efficacy in the clinical trial data because of dose-limiting toxicity (e.g. skin rash and diarrhea) caused by the loss of selectivity over wild-type EGFR ($EGFR^{WT}$).[17, 18]

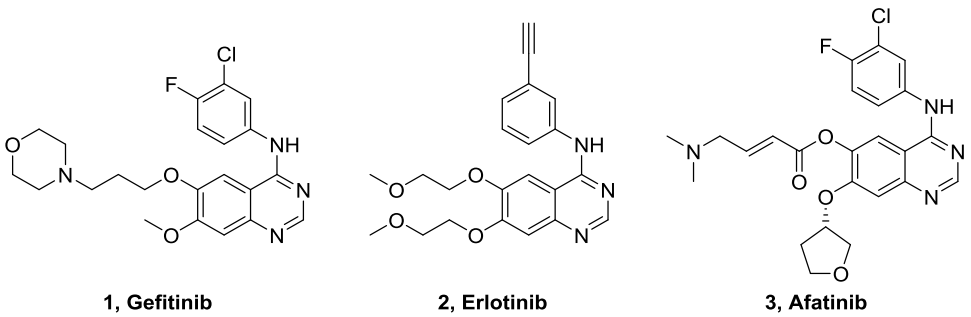

Fig. 1. The structures of the first- and second-generation EGFR-TKIs

To conquer the shortcoming of second-generation EGFR-TKIs, researchers developed third-generation inhibitors with high potency against T790M resistant mutation but sparing $EGFR^{WT}$ activity. The strategy of employing an electrophilic group capable of forming a C-S covalent bond with the conserved Cys797 residue was still used in drug design and optimization. In the past few years, a family of 2-aminopyrimidine-based compounds, including osimertinib (AZD9291)[19-21], rociletinib (CO-1686)[22], olmutinib (HM61713)[23], avitinib (AC0010)[24], PF-06747775[25] and PF-06459988[26] have been researched to overcome T790M mutation-related resistance (Fig. 2). These inhibitors not only effectively target activated mutations and the T790M resistant mutation but also display better selectivity over $EGFR^{WT}$. For its precise biological properties, osimertinib was approved by FDA in 2015 for the treatment of T790M patients. The progress of 2-aminopyrimidine-based EGFR-T790M inhibitors has been comprehensively summarized.[27-31]

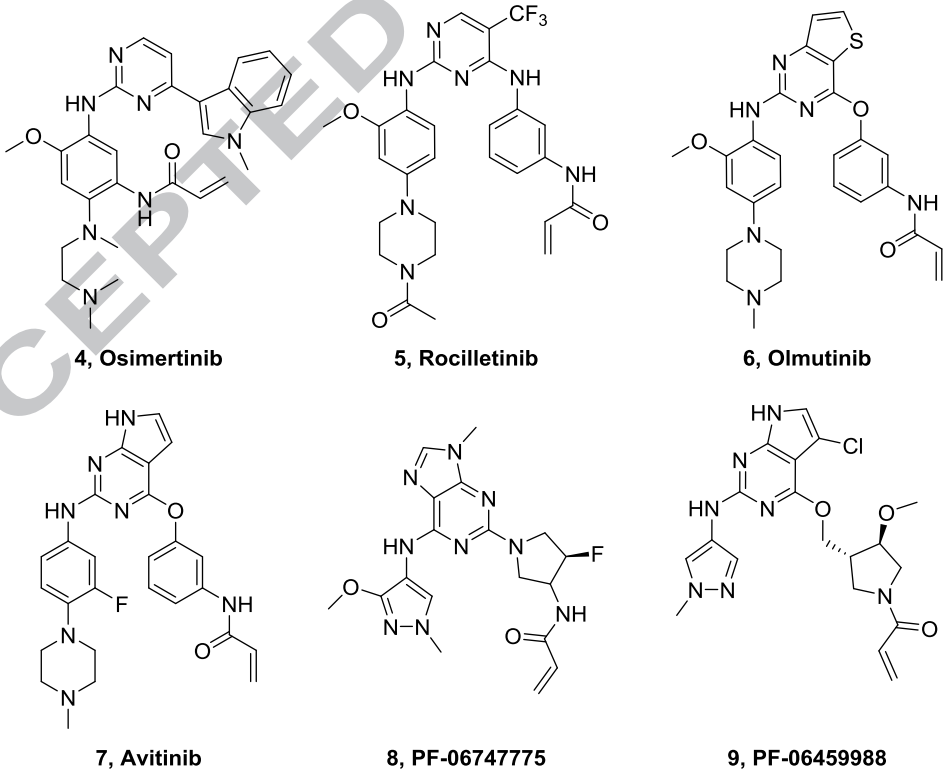

Fig. 2. The structures of the third-generation EGFR-TKIs

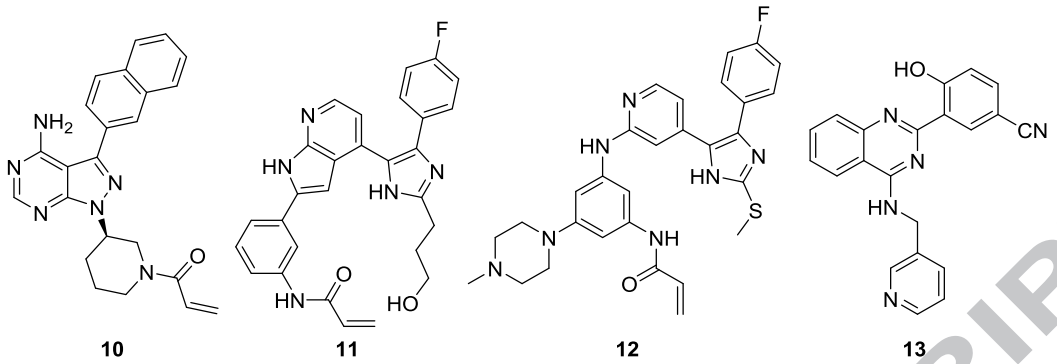

10 11 12 13

Fig. 3. The structures of new generation EGFR-TKIs with potency to EGFR C797S

Despite great success of third-generation EGFR-TKIs, acquired resistance remains a significant clinical issue in NSCLC treatment. Resistance mechanisms of the third-generation EGFR-TKIs have been summarized.[27, 30] Among those possible mechanisms, triple mutation C797S in EGFR accounts for more than 20%. Recently, compounds **10**[32, 33], **11**[34, 35] **12**[36] and **13**[37] were discovered as a new generation EGFR-TKIs to combat the C797S-mediated resistance. Lately, we demonstrated that 2,4,6-trisubstitued pyrido[3,4-*d*]pyrimidine[38] and 2,9-disubstituted 8-phenylthio/phenylsulfinyl-9*H*-purine[39] derivatives could serve as reversible EGFR-TKIs with potent activities on $EGFR^{L858R/T790M/C797S}$. Among those novel compounds, compound **14** (Fig. 4) displayed strong activity against $EGFR^{L858R/T790M/C797S}$ with IC_{50} value of 7.2 nM. Compared with the third-generation EGFR inhibitors, compounds **10-12** and **14** incorporate a 2-naphthyl or 4-fluorophenyl to occupy the back hydrophobic pocket (BHP) formed by gatekeeper Met790 and the side chain of Lys745, yielding potent activity due to the hydrophobic interaction.

The innovation of drug structure is crucial in medicinal chemistry research. It is of great value to develop more active and selective EGFR-T790M small molecule inhibitors with a novel chemical skeleton. In an effort to acquire more effective EGFR-T790M inhibitors based on reversible inhibitor **14**, (i) we introduced acrylamide warhead with moderate chemical reactivity as Michael acceptor (marked in pink) to form the C-S covalent bond with Cys797 residue[25, 26]; (ii) aminopyrrolidine and aminopiperidine with higher sp^3 character was used as the linker of pyrido[3,4-*d*]pyrimidine scaffold and warhead to achieve decreased melting point, improved solubility and increased activity and selectivity[40-43]; (iii) in terms of orientation and geometry, the rigid R^1 phenylamino group was introduced to insert

BHP for lipophilic interactions. Herein, we describe the synthesis and biological activities evaluation of pyrido[3,4-*d*]pyrimidine derivatives bearing flexible linker and acrylamide warhead to target EGFR and overcome T790M resistance.

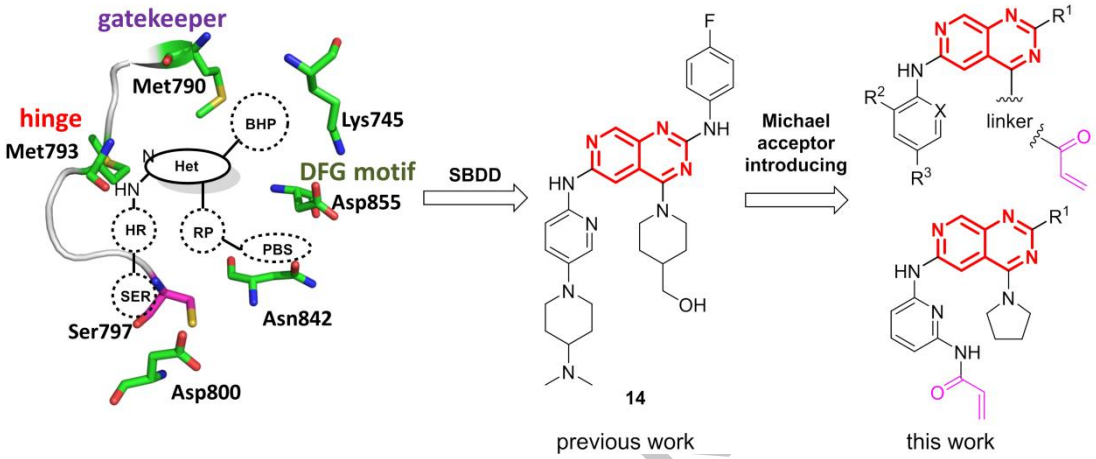

Fig. 4. Design of novel irreversible EGFR-TKIs containing pyrido[3,4-*d*]pyrimidine scaffold. **Het**, heterocyclic scaffold; **BHP**, back hydrophobic pocket; **HR**, hydrophobic region; **SER**, solvent exposed region; **RP**, ribose pocket; **PBS**, phosphate binding site.

2. Results and discussion

2.1. Chemistry

The synthetic route for compounds **20a-d** was outlined in Scheme 1. Commercially available 5-amino-2-chloroisonicotinic acid was used as the starting material. The heating of the starting material with formamidine acetate produced intermediate **15** in a solvent-free condition. Intermediate **15** was converted into 4,6-dichloropyrido[3,4-*d*]pyrimidine (**16**) by the reaction with thionyl chloride. Depending on distinct difference in reactivity, 4-chloride in intermediate **16** was substituted by pyrrolidine at room temperature to yield intermediate **17**. The Boc protecting group was removed by TFA, and the free amino group reacted with acryloyl chloride to obtain intermediate **18**. With the aid of Buchwald-Hartwig amination, treatment of intermediate **18** with substituted aniline or 5-substituted pyridin-2-amine yielded title compounds **20a-d**.

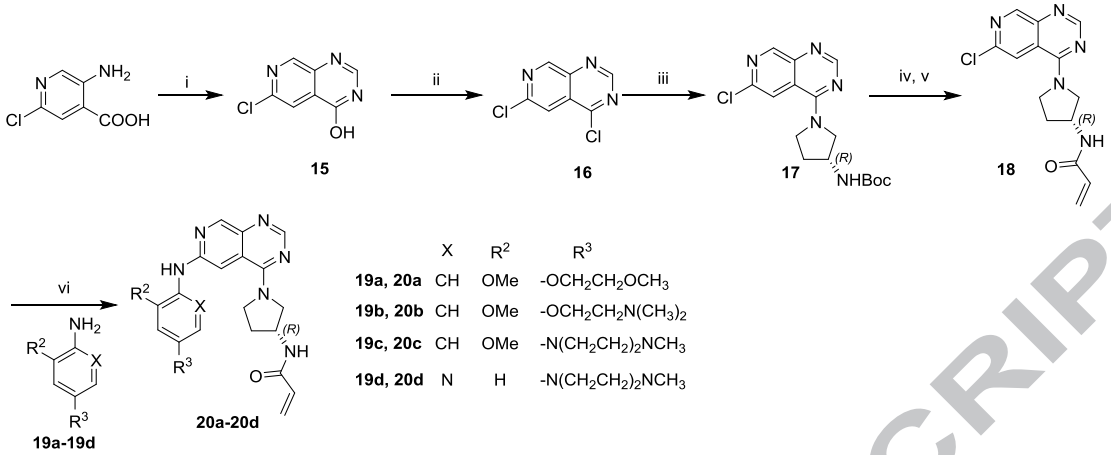

Scheme 1. Synthetic route of compounds **20a-d**. Reagents and conditions: (i) formamidine acetate, 160 °C, 0.5 h, 90.4%; (ii) $SOCl_2$, DMF(cat.), reflux, 4 h; (iii) amine, DIPEA, THF, rt, 2 h, 65.1%, over two steps; (iv) TFA, DCM, rt, 1.5 h; (v); acryloyl chloride, TEA, DCM, 0 °C–rt, 2 h, 79.8%, over two steps; (vi) $Pd(OAc)_2$, X-phos, Cs_2CO_3, 1,4-dioxane, reflux, 4 h, 56.4%–83.6%.

The synthetic route for compounds **25a-h** was depicted in Scheme 2. 2,4,6-Trichloropyrido[3,4-*d*]pyrimidine (**21**) was prepared from 5-amino-2-chloroisonicotinic acid as we reported.[38] Depending on distinct difference in reactivity, three chlorine atoms at the 4,2,6-position in **21** were successively replaced by amines. Intermediates **22a-h** were obtained by stirring the mixture of intermediate **21**, DIPEA and different amines in THF. The Boc group in **22a-h** was removed by TFA, and the free amino group reacted with acryloyl chloride to obtain intermediates **23a-h**. Intermediates **24a-h** were produced by refluxing intermediates **23a-h** and substituted aniline in 2-butanol. With the aid of Buchwald-Hartwig amination, treatment of intermediates **24a-h** with 5-substituted pyridin-2-amine yielded title compounds **25a-h**.

To boost the structural diversity of the title compounds, 6-(acrylamidopyridin-2-amino)-4-(pyrrolidin-1-yl)pyrido[3,4-*d*]pyrimidines **29a-g** (Scheme 3) were synthesized with similar approach.

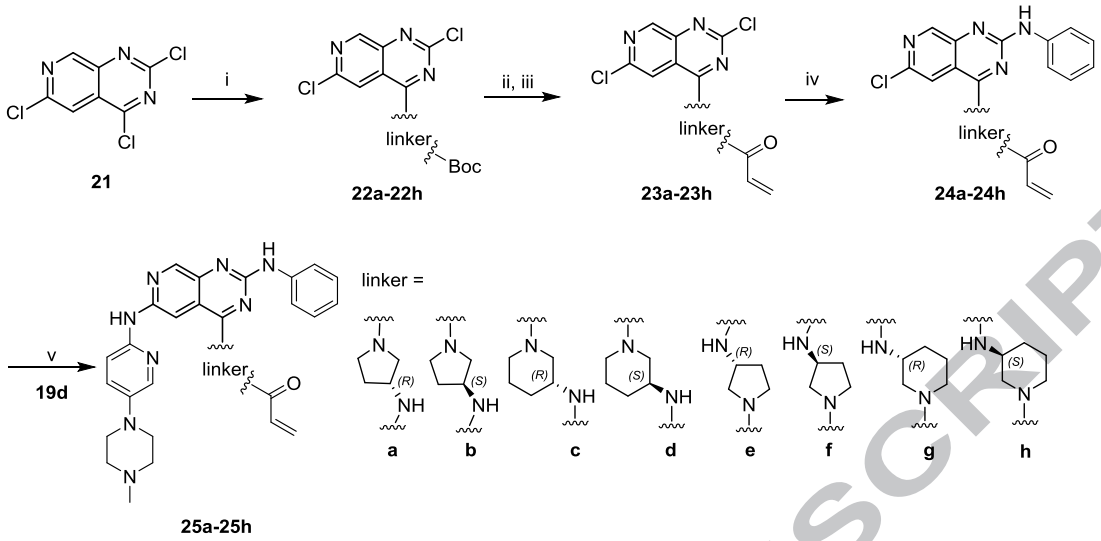

Scheme 2. Synthetic route of compounds **25a-h**. Reagents and conditions: (i) amines, DIPEA, THF, rt, 1–2 h, 72.0%–100%; (ii) TFA, DCM, 0.5 h–2 h; (iii) acryloyl chloride, DIPEA, DCM, 0 °C–rt, 2 h–4 h, 24.9%–79.2%, over two steps; (iv) anilines, *p*-TsOH, 2-butanol, reflux, 2 h–4 h, 64.4%–100%; (v) $Pd(OAc)_2$, X-phos, Cs_2CO_3, 1,4-dioxane, reflux, 2 h–4 h, 23.7%–67.7%.

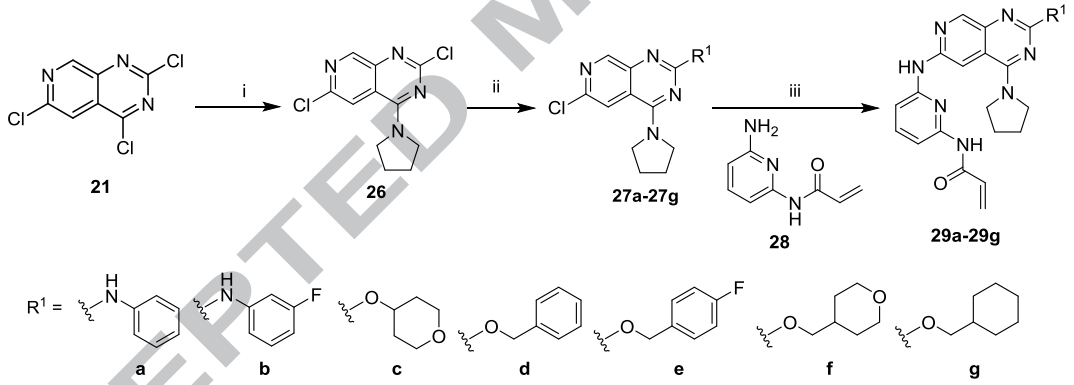

Scheme 3. Synthesis route of compounds **29a-g**. Reagents and conditions: (i) amines, DIPEA, THF, rt, 0.5 h, 90.9%; (ii) for **27a** and **27b**, anilines, *p*-TsOH, 2-butanol, reflux, 2 h, 91.8–99.2%; for **27c-g**, alcohols, NaH, THF, rt, 2 h, 98.0%–100%; (v) $Pd(OAc)_2$, X-phos, Cs_2CO_3, 1,4-dioxane, reflux, 2 h–4 h, 17.6%–41.9%.

2.2. Biological evaluations

2.2.1. The antiproliferative activity *in vitro*

By employing the 3-[4,5-dimethylthiazol-2-yl]-2,5-diphenyl-*2H*-tetrazolium bromide (MTT) assay, we first evaluate the antiproliferative activities of synthesized compounds against human epithelial carcinoma cell lines including A549 ($EGFR^{WT}$), HCC827 (harboring activated mutant $EGFR^{Del\ E746\text{-}A750}$) and H1975 (drug-resistant, carrying $EGFR^{L858R/T790M}$). The third-generation EGFR inhibitor osimertinib was used

as the positive drug. The results of compounds **20a-d** and **25a-h** were listed in Table 1.

Table 1. Antiproliferative effects of compounds **20a-d** and **25a-h** (Mean ± SD, n = 3)

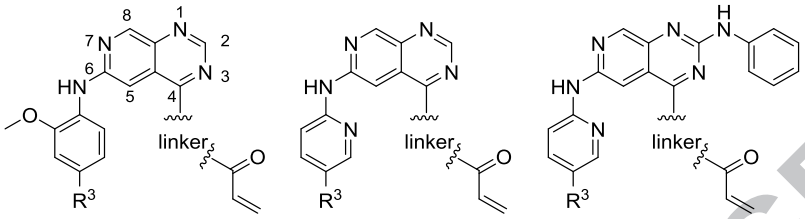

20a-c **20d** **25a-h**

Compds	linker	R^3	IC_{50} (μM)		
			HCC827	H1975	A549
20a	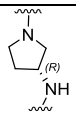	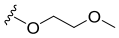	>10[a]	ND[b]	ND
20b	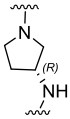	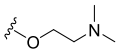	>10	ND	ND
20c	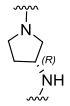	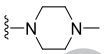	>10	ND	ND
20d	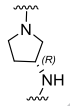		3.52 ± 0.16	>10	ND
25a	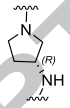	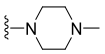	0.020 ± 0.003	1.44 ± 0.06	1.19 ± 0.33
25b	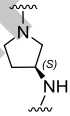	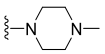	0.069 ± 0.013	0.85 ± 0.16	0.64 ± 0.13
25c	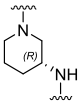	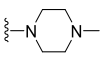	0.054 ± 0.023	1.75 ± 0.42	0.81 ± 0.02
25d	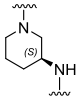	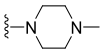	0.073 ± 0.005	1.40 ± 0.02	0.81 ± 0.26
25e	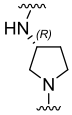	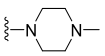	0.17 ± 0.01	0.44 ± 0.08	0.65 ± 0.10
25f	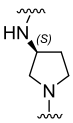	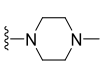	0.27 ± 0.02	0.86 ± 0.25	1.67 ± 0.40
25g	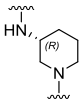	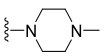	0.16 ± 0.02	1.40 ± 0.24	0.81 ± 0.05

25h	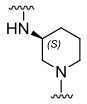	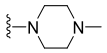	0.025 ± 0.005	0.49 ± 0.08	0.99 ± 0.04
osimertinib			0.027 ± 0.01	0.019 ± 0.008	0.53 ± 0.09

[a] inhibition rate < 50% at 10 μM; [b] ND, not determined.

To explore the effect of substituent at the 6-position of pyrido[3,4-*d*]pyrimidine scaffold, we first synthesized compounds **20a-c**. Disappointingly, no significant antiproliferative activities against HCC827 cells were observed in compounds **20a-c**. We suspected that it is difficult for **20a-c** to maintain pharmacophoric conformation owing to the steric repulsion between the hydrogen atom at 5-position of pyrido[3,4-*d*]pyrimidine and the hydrogen atom at 2-position of aniline. To overcome the problem of steric clash, pyridin-2-yl was used to replace phenyl and compound **20d** were obtained. In contrast with compounds **20a-c**, compound **20d** displayed improved antiproliferative activity against HCC827 cells with IC_{50} value of 3.52 μM. The results indicated that the replacement of the phenyl with pyridin-2-yl was proved to be effective in the promotion of antiproliferative activity. This finding is consistent with our previous study of reversible EGFR-TKIs.[38] Subsequently, to further enhance the activity, compounds **25a-h** with a phenylamino group at 2-position of scaffold were synthesized. Compound **25a** displayed potent activity against HCC827 with the IC_{50} value of 0.020 μM, which is more than 170-fold higher than compound **20d**. Obviously, 2-phenylamino moiety is very important to improve antiproliferative activity. Compounds **25a** and **25b** with a 3-(acrylamido)pyrrolidin-1-yl group attached to the 4-position of pyrido[3,4-*d*]pyrimidine scaffold exhibited potent antiproliferative effects on HCC827 cells. While in compounds **25e** and **25f** with a 1-acrylamidopyrrolidin-3-yl-amino group attached to the 4-position of pyrido[3,4-*d*]pyrimidine scaffold, only moderate antiproliferative effects were observed. In these cases, (*R*)-configuration of chiral carbon is favorable for antiproliferative effect. Compounds **25c** and **25d** with a 3-(acrylamido)piperidin-1-yl group attached to the 4-position of pyrido[3,4-*d*]pyrimidine scaffold exhibited potent antiproliferative effects on HCC827 cells. Compounds **25h** with a (*S*)-1-(acrylamido)piperidin-3-yl group attached to the 4-position of pyrido[3,4-*d*]pyrimidine scaffold exhibited potent antiproliferative effects on HCC827 cells (IC_{50} = 0.025 μM) and mild antiproliferative effects on H1975 cells (IC_{50} = 0.49 μM). Moreover, compounds **25a-h** showed more potent activities against HCC827

than the other cells.

To extend the diversity of compound structures and further study structure-activity relationship (SAR), we moved the acrylamide moiety from 4-postion to 6-postion of pyrido[3,4-*d*]pyrimidine scaffold to produce compounds **29a-g**. However, compared with compounds **25a-h** and positive control, these compounds showed a significant drop in the cell-based activity (Table 2). Only compounds **29c** and **29f** displayed moderate activity against HCC827 cells with IC_{50} value of 2.74 μM and 8.70 μM, respectively. We noticed that compounds **29a-g** showed poorer solubility than compounds **25a-h** due to the lack of 4-methylpiperazin-1-yl. And not only that, the polar 4-methylpiperazin lacking in compounds **29a-g** can stretch into solvent exposed region (SER), which hinted that the polar group may be helpful for activity. The results indicated that 6-acrylamido pyridine-2-ylamino at the 6-position of pyrido[3,4-*d*]pyrimidine scaffold was not suitable.

Table 2. Antiproliferative effects of compounds **29a-g** (Mean ± SD, n = 3)

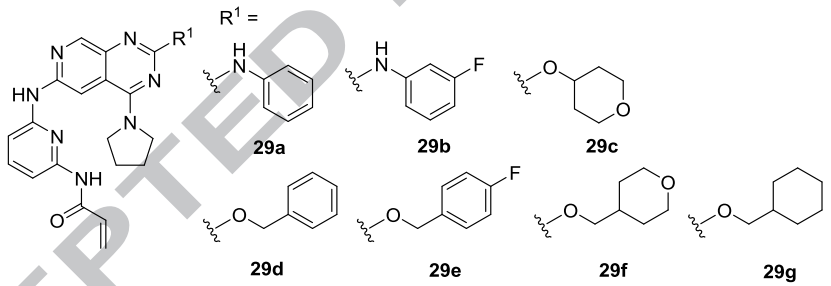

Compds	IC_{50} (μM)
	HCC 827
29a	> 10[a]
29b	> 10
29c	2.74 ± 0.58
29d	> 10
29e	> 10
29f	8.70 ± 2.10
29g	> 10
osimertinib	0 027 ± 0.01

[a] inhibition rate < 50% at 10 μM.

2.2.2. EGFR kinase activities assay

Compounds **25a-h**, the active inhibitors against HCC827 cells, were selected to determine their kinase inhibitory activity against EGFR to verify the mechanism of

antiproliferative activities. Osimertinib was used as the positive control. The data were listed in Table 3. We can see that the selected compounds **25a-h** displayed very potent activities against activating mutation $EGFR^{L858R}$ with nanomolar range inhibitory activity (IC_{50} values from 1.7 nM to 14.2 nM). Meanwhile, compounds **25a**, **25b** and **25h** also showed strong inhibitory activity on $EGFR^{L858R/T790M}$ with the IC_{50} values of 36.6, 26.5 and 23.3 nM, respectively. Moreover, weak activities against triple mutation $EGFR^{L858R/T790M/C797S}$ were observed in **25b** (IC_{50} = 285.0 nM) and **25h** (IC_{50} = 582.2 nM). Compared to reversible inhibitor **14** we have previously descried, the irreversible compounds **25a-h** showed weak inhibitory activity against $EGFR^{L858R/T790M/C797S}$ in spite of introduction of acrylamide. Indeed, the acrylamide moiety is not very important for the activity against $EGFR^{L858R/T790M/C797S}$ but crucial for the T790M inhibition. The results of kinase activities assay also showed that compounds **25a-h** and osimertinib exhibited potent inhibitory activity against $EGFR^{WT}$ at the same test conditions. It can be seen that the kinase inhibitory activities of tested compounds are consistent with the effects on two selected cell lines HCC827 and H1975 harboring different EGFR types.

Table 3. Enzymatic activities of compounds against different types of EGFR (n = 2)

Compds	IC_{50} (nM)			
	WT	L858R	L858R/T790M	L858R/T790M/C797S
25a	2.7	4.7	36.6	ND[a]
25b	1.5	3.2	26.5	285.0
25c	5.4	6.5	163.7	> 500[b]
25d	12.0	14.2	361.1	> 500
25e	3.3	4.6	106.4	> 500
25f	9.9	10.8	238.1	> 500
25g	4.7	4.5	130.2	> 500
25h	1.9	1.7	23.3	582.2
osimertinib	0.9	1.2	2.4	109.0
	< 0.5[c]	< 0.5[c]	< 0.5[c]	
	2[d]	1[d]	< 1[d]	77[d]

[a] ND, not determined; [b] Inhibition rate < 50% at 500 nM; [c] The data reported by Gunther[33]; [d] The data reported by Engel[31].

2.2.3. Western blotting assay

To further verify the mechanism of the antiproliferative activity of compound **25h**, Western blotting assay was employed to characterize inhibition of p-EGFR in HCC827 and H1975 cell lines. As depicted in Fig. 5, compound **25h** showed

significant suppression of p-EGFR in HCC827 at all tested concentrations range (Fig. 5A) while showed different suppression of p-EGFR in H1975 in a dose-dependent manner (Fig. 5B). In addition, the inhibition of phosphorylation of EGFR in HCC827 and H1975 is consistent with antiproliferative activity in MTT assay.

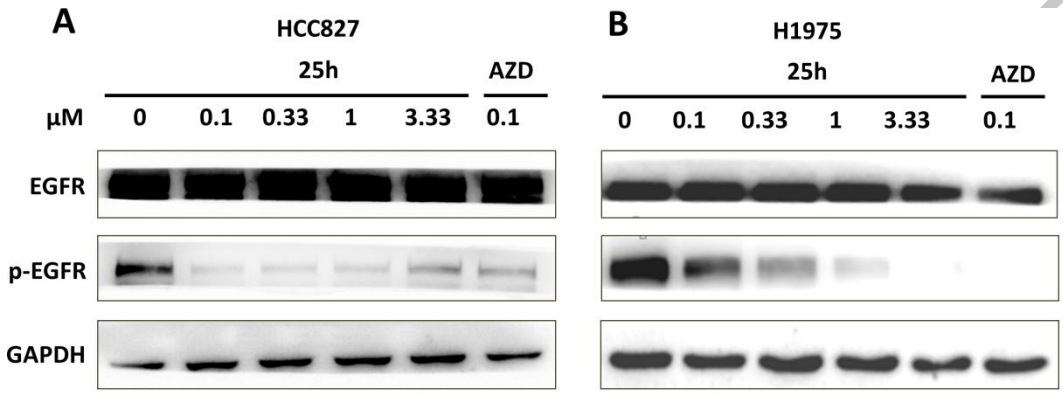

Fig. 5. Effects of compound **25h** on EGFR signaling in HCC827 (A) and H1975 (B) cells. Cells were treated with the indicated concentrations for 8 h.

2.2.4. Cell apoptosis assay

To characterize whether compound **25h** can induce cell apoptosis, the annexinV/propidium iodide (PI) biparametric cytofluorimetric assay was performed on HCC827 cells. As illustrated in Fig. 6, the percentages of apoptotic cells for osimertinib and **25h** at 3 μM were 76.38% and 75.84%, respectively, which indicated that compound **25h** could significantly induce the apoptosis of HCC827 cells.

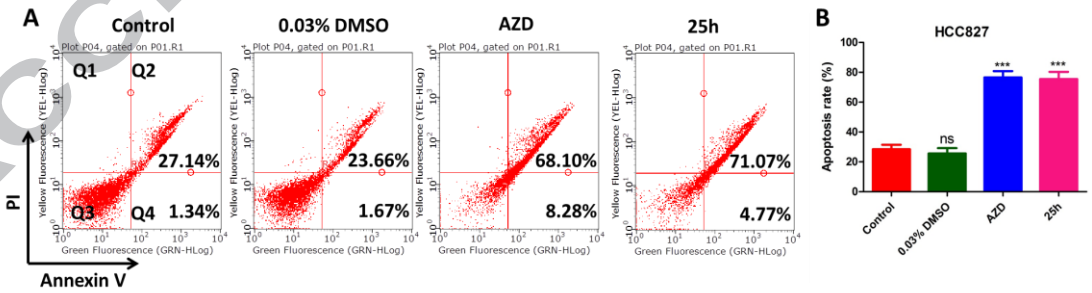

Fig. 6. The apoptosis effect of compound **25h** on HCC827 cells. (A) Without drug or DMSO treat (control) and after treated with 0.03% DMSO, 3 μM of AZD (osimertinib) and **25h** for 24 h. The upper left quadrant Q1 represented necrotic cells, the upper right quadrant Q2 represented for late apoptotic cells, the low left quadrant Q3 represented live cells and the low right quadrant Q4 represented for early apoptotic cells. Results are mean of three independent experiments. (B) The apoptosis rate was the sum of Q2+Q4. Data are the means ± SD of values from three independent

experiments (ns, not significant vs control; *** $p < 0.001$ vs 0.03% DMSO).

2.2.5. Anticancer effect *in vivo*

Finally, the most promising inhibitor **25h**, with potent inhibitory activity against $EGFR^{L858R}$ and antiproliferative effect on HCC827, was evaluated for its antitumor efficacy in HCC827 xenograft mouse model *in vivo*. According to reported data of related third-generation EGFR-TKIs[43-46], oral administration doses of **25h** were selected 10 mg/kg and 50 mg/kg. In the HCC827 xenograft model, mice (n = 5-6/group) were oral dosed once daily for 20 consecutive days. As depicted in Fig. 7A, **25h** significantly inhibited the tumor growth at the dose of 10 mg/kg (TGI = 60.6%) and 50 mg/kg (TGI = 86.5%) compared with the vehicle group. In addition, during the course of the experiment, compound **25h** did not cause significant body weight loss and no mortality of mice was observed (Fig. 7C), suggesting that **25h** was tolerated well with low toxicity at those doses.

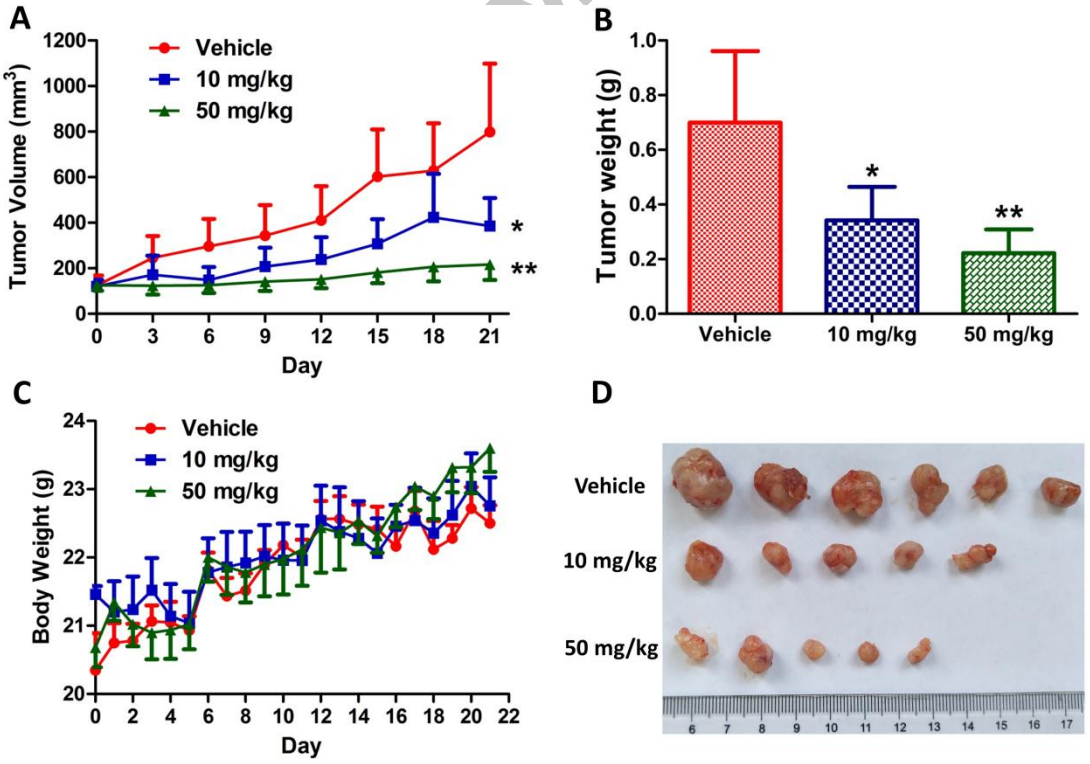

Fig. 7. *In vivo* antitumor efficacy of **25h** in HCC827 xenograft mouse model at 10 mg/kg and 50 mg/kg. (A) Tumor volumes. (B) Tumor weights. (C) Body weight of mice. (D) Images of the tumor collected from the mice on d21. All data represent mean ± SEM. (* $p < 0.05$, ** $p < 0.01$ *vs* vehicle).

2.2.6. Molecular docking study

In order to explore the binding mode of our compounds, Sybyl-X 2.0 software was used to dock **20d**, **25a** and **25h** into ATP binding site of $EGFR^{T790M}$ (PDB code 2JIU).[8] The results were depicted in Fig. 8. As the foremost pharmacophore, the nitrogen atom at 7-position of pyrido[3,4-*d*] pyrimidine and the hydrogen atom from aminopyridine at 6-position formed two vital hydrogen bonds with Met793 in the hinge region. Hydrogen atom in aniline at 2-position of pyridopyrimidine scaffold formed a hydrogen bond with gatekeeper residue Met790. The aminopyrrolidine or aminopiperidine moiety at 4-position occupied the ATP ribose pocket and generated Van der Waals interaction with Phe856 and Asp855 from the Asp-Phe-Gly (DFG) motif. In potent inhibitors **25a** and **25h**, aniline at 2-position of pyrido[3,4-*d*]pyrimidine inserted into the BHP (marked in red circle) (Fig. 8E/8F and Fig. 8H/I) to form hydrophobic interactions. However, owing to the lack of aniline to occupy the BHP (Fig. 8B/C), compound **20d** only displayed weak activity on HCC827 cells. Those findings implied that the hydrophobic interaction formed by BHP with inhibitor was closely linked to inhibitory activity. In addition, the distance (2.7 Å) of Cys797 toward acrylamide moiety in compound **25h** (Fig. 8H) indicated the potential possibility of forming covalent bond, which hinted **25h** could serve as irreversible EGFR inhibitor. Obviously, the docking results further verified our design strategy.

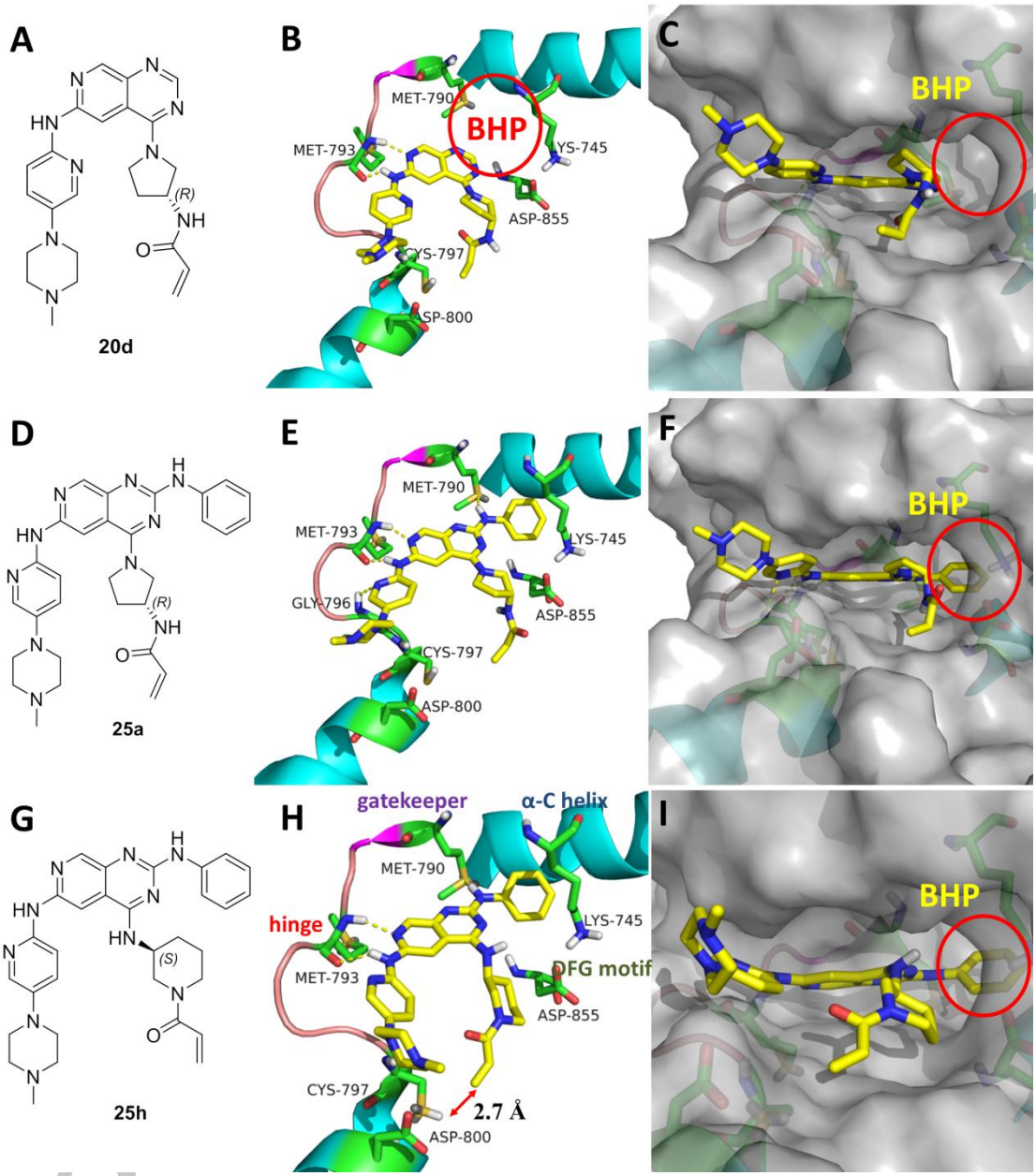

Fig. 8. (A) Structure of **20d**, (B) docking result of **20d** with EGFR^{T790M} and (C) gray surface representation of **20d** docked into ATP-binding site. (D) Structure of **25a**, (E) docking result of **25a** with EGFR^{T790M} and (F) gray surface representation of **25a** docked into ATP-binding site. (G) Structure of **25h**, (H) docking result of **25h** with EGFR^{T790M} and (I) gray surface representation of **25h** docked into ATP-binding site. Hydrogen bonds are indicated as yellow dashed lines. inhibitors (yellow) and key protein residues (green) are highlighted in stick form. Clear hydrogen bond interactions with Met793, Met 790 and Gly 796 are observed. Red arrow indicates the distance (2.7 Å) of Cys797 and acrylamide moiety in **25h**. Red circles represent the back hydrophobic pocket (BHP). Some parts of the protein are omitted for clarity.

3. Conclusions

In summary, we demonstrated that the 2,4-disubstituted 6-(5-substituted

pyridin-2-amino)pyrido[3,4-*d*]pyrimidine derivatives can serve as effective EGFR inhibitors and potent anticancer agents. The most promising compound **25h** inhibited HCC827 and H1975 cells growth with the IC_{50} values of 0.025 μM and 0.49 μM, respectively. Meanwhile, **25h** displayed potent inhibitory activity against the $EGFR^{L858R}$ (IC_{50} = 1.7 nM) and $EGFR^{L858R/T790M}$ (IC_{50} = 23.3 nM). Further experiments indicated that **25h** could suppress EGFR phosphorylation in HCC827 and H1975 cell lines and significantly induce the apoptosis of HCC827 cells. Additionally, compound **25h** at 50 mg/kg could remarkably inhibit cancer growth in established HCC827 nude mouse xenograft model *in vivo*.

4. Experimental protocols

4.1. Chemistry and chemical methods

Unless specified otherwise, all the starting materials, reagents and solvents were commercially available. All reactions were monitored by thin-layer chromatography (TLC) on silica gel plates (GF-254) and visualized with UV light (254 nm and 365 nm). All melting points were determined on a Shanghai micro melting-point instrument (SGW® X-4B) and the thermometer was uncorrected. NMR spectra were recorded on a 400 Bruker NMR spectrometer with tetramethylsilane (TMS) as an internal reference. All chemical shifts are reported in parts per million (ppm). The following abbreviations were used to describe peak splitting patterns when appropriate: s (singlet), d (doublet), t (triplet), m (multiplet), br (broad signal), dd (doublet of doublets). Coupling constants (*J*) are expressed in hertz unit (Hz). Mass spectrum (MS) was obtained by ESI-MS (Skyray instrument LC-MS 1000). High resolution mass spectrum (HRMS) was obtained via using electrospray ionization (positive mode) on an Ultra performance liquid chromatography-Quadrupole-time of flight Mass Spectrometer (WATERS I-Class VION IMS Q-TOF). Polarimeter (IP-digi300EDU, Shanghai InsMark Instrument Technology Co., Ltd) was used to obtain specific rotations when a sufficient sample was available. Specific rotations based on the equation $[\alpha] = (100 \cdot \alpha)/(l \cdot c)$ was reported as $[\alpha]_D^{20}$ (c 2.0, MeOH, where the concentration c is in g/l00 mL and the path length l is in decimeters)..

4.1.1. 6-Chloropyrido[3,4-*d*]pyrimidin-4-ol (**15**)

The mixture of 5-amino-2-chloroisonicotinic acid (5.00 g, 29.07 mmol) and formamidine acetate (6.00 g, 58.14 mmol) was stirred at 160 °C for 0.5 h, cooled,

water (100 mL) was added. The mixture was refluxed under vigorous stirring for 20 min, cooled again. The precipitate formed was collected, washed with water and dried to give 4.74 g intermediate **15** as off-white power. Yield 90.4%. mp > 320 °C. MS m/z (ESI) 182.4 $[M+H]^+$.

4.1.2. *Tert*-butyl (*R*)-(1-(6-chloropyrido[3,4-*d*]pyrimidin-4-yl)pyrrolidin-3-yl) carbamate (**17**)

The mixture of intermediate **15** (2.00 g, 11.01 mmol), $SOCl_2$ (20 mL) and DMF (5 drops) was refluxed for 4 h. The remaining $SOCl_2$ was distilled off. The residue was cooled, suspended with water, extracted with ethyl acetate (30 mL×3). The organic layer was separated, washed with saturated NaCl solution, dried over anhydrous Na_2SO_4 and concentrated to give 4,6-dichloropyrido[3,4-*d*]pyrimidine (intermediate **16**) as light yellow solid. Intermediate **16** was dissolved in isopropanol (25mL), DIPEA (3 mL, 16.52 mmol) and tert-butyl (*R*)-pyrrolidin-3-ylcarbamate (2.05 g, 11.01 mmol) was added. The mixture was stirred at room temperature for 2 h. The solvent was removed under reduced pressure. The residue was suspended with water and extracted with ethyl acetate (25 mL×3). The organic phase was washed with saturated NaCl solution, dried over anhydrous Na_2SO_4 and concentrated. The crude product was suspended in cooled ethanol (15 mL) and filtered to give intermediate **17** as light yellow power. Yield 2.50 g, 65.1%, over two steps. mp 89.5–91.4 °C. ^{1}H NMR (400 MHz, $CDCl_3$) δ 9.09 (s, 1H, Ar-H), 8.65 (s, 1H, Ar-H), 7.90 (s, 1H, Ar-H), 4.95–4.65 (m, 1H, NH), 4.53–4.30 (m, 1H, CH), 4.24–3.95 (m, 3H, NCH_2), 3.90–3.75 (m, 1H, NCH_2), 2.40–2.30 (m, 1H, CH_2), 2.18–2.08 (m, 1H, CH_2), 1.46 (s, 9H, $C(CH_3)_3$). MS m/z (ESI) 350.7 $[M+H]^+$.

4.1.3. (*R*)-*N*-(1-(6-chloropyrido[3,4-*d*]pyrimidin-4-yl)pyrrolidin-3-yl)acrylamide (**18**)

To the solution of intermediate **17** (200 mg, 0.59 mmol) in DCM (8 mL), TFA (2 mL) was added, and the mixture was stirred at room temperature for 1.5 h. The solvent was removed under reduced pressure to get crude amine which was used for the next step without furfure purification. To the mixture of the amine and DIPEA (0.3 mL, 1.77 mmol) in DCM (15 mL), acryloyl chloride (60 μL, 0.71 mmol) diluted with DCM (5 mL) was added dropwise. The mixture was stirred at room temperature and for 2 h, quenched with aqueous $NaHCO_3$ solution and extracted with DCM (30

mL×2). The organic layer was washed with saturated NaCl solution, dried over anhydrous Na_2SO_4, and concentrated under reduced pressure to give intermediate **18** as white solid. Yield 150 mg, 79.8%, over two steps. mp 232.8–235.3 °C. ^{1}H NMR (400 MHz, DMSO-d_6) δ 8.95 (s, 1H, Ar-H), 8.60 (s, 1H, Ar-H), 8.44 (d, J = 6.4 Hz, 1H, NH), 8.09 (s, 1H), 6.25–6.09 (m, 2H, CH=CH_2), 5.62 (dd, J = 9.6, 2.7 Hz, 1H, CH=CH_2), 4.53–4.44 (m, 1H, CH), 4.26–3.76 (m, 4H, NCH_2), 2.30–2.18 (m, 1H, CH_2), 2.08–1.95 (m, 1H, CH_2). MS m/z (ESI) 320.7 $[M+H]^+$.

4.1.4. Synthesis of intermediates **19a-d**

2-Methoxy-4-(2-methoxyethoxy)aniline (**19a**), 4-(2-(dimethylamino)ethoxy)-2-methoxyaniline (**19b**) and 2-methoxy-4-(4-methylpiperazin-1-yl)aniline (**19c**) were synthesized from 4-fluoro-2-methoxy-1-nitrobenzene.[47] 5-Bromo-2-nitropyridine was used as starting material to prepare 5-(4-methylpiperazin-1-yl)pyridine-2-amine (**19d**).[48]

4.1.5. 2,4,6-Trichloropyrido[3,4-*d*]pyrimidine (**21**)

Intermediate **21** was prepared from 5-amino-2-chloroisonicotinic acid as we previously reported.[38]

4.1.6. General procedure for the synthesis of intermediates **22a-h**

To a mixture of intermediate **21** (1 mmol) and DIPEA (1.5 mmol) in THF, amine (1.1 mmol) was added under stirring. The mixture was stirred for about 0.5 h–2 h at room temperature. The solvent was removed under reduced pressure and the residue was suspended in water. The solid was collected by filtration, washed with water and dried to obtain intermediates **22a-h**.

4.1.6.1. tert-butyl (*R*)-(1-(2,6-dichloropyrido[3,4-*d*]pyrimidin-4-yl)pyrrolidin-3-yl) carbamate (**22a**)

Light yellow solid. Yield 78.7%. mp 95.6–97.8 °C. ^{1}H NMR (400 MHz, $CDCl_3$) δ 8.98 (s, 1H, Ar-H), 7.89 (s, 1H, Ar-H), 4.76 (s, 1H, NH), 4.51–4.36 (m, 1H, NCH_2), 4.25–4.01 (m, 3H, NCH_2), 3.90–3.81 (m, 1H, CH), 2.41–2.07 (m, 2H, CH_2), 1.45 (s, 9H, $(CH_3)_3$). MS m/z (ESI) 384.2 $[M+H]^+$.

4.1.6.2. tert-butyl (*S*)-(1-(2,6-dichloropyrido[3,4-*d*]pyrimidin-4-yl)pyrrolidin-3-yl) carbamate (**22b**)

Light yellow solid. Yield 100.0%. mp 101.3–103.5 °C. ^{1}H NMR (400 MHz, $CDCl_3$) δ 8.97 (s, 1H, Ar-H), 7.89 (s, 1H, Ar-H), 4.76 (s, 1H, NH), 4.52–4.36 (m, 1H, NCH_2), 4.26–3.98 (m, 3H, NCH_2), 3.92–3.79 (m, 1H, CH), 2.43–2.29 (m, 1H, CH_2), 2.21–1.95 (m, 1H, CH_2), 1.45 (s, 9H, $(CH_3)_3$). MS m/z (ESI) 384.2 $[M+H]^+$.

4.1.6.3. tert-butyl (*R*)-(1-(2,6-dichloropyrido[3,4-*d*]pyrimidin-4-yl)piperidin-3-yl) carbamate (**22c**)

Light yellow solid. Yield 89.3%. mp 209.3–212.6 °C. ^{1}H NMR (400 MHz, $CDCl_3$) δ 9.03 (s, 1H, Ar-H), 8.05 (s, 1H, Ar-H), 4.95–4.63 (m, 1H, NH), 4.38–4.17 (m, 2H, NCH_2), 3.98–3.75 (m, 1H, CH), 3.57–3.41 (m, 2H, NCH_2), 2.17–2.05 (m, 1H, CH_2), 2.00–1.94 (m, 1H, CH_2), 1.85–1.77 (m, 1H, CH_2), 1.74–1.63 (m, 1H, CH_2), 1.43 (s, 9H, $(CH_3)_3$). MS m/z (ESI) 398.0 $[M+H]^+$.

4.1.6.4. tert-butyl (*S*)-(1-(2,6-dichloropyrido[3,4-*d*]pyrimidin-4-yl)piperidin-3-yl) carbamate (**22d**)

Light yellow solid. Yield 84.3%. mp 204.9–206.2 °C. ^{1}H NMR (400 MHz, $CDCl_3$) δ 9.05 (s, 1H, Ar-H), 8.06 (s, 1H, Ar-H), 4.80 (s, 1H, NH), 4.31–4.27 (m, 2H, NCH_2), 3.89 (s, 1H, CH), 3.47–3.43 (m, 2H, NCH_2), 2.04–2.00 (m, 2H, CH_2), 1.79–1.74 (m, 2H, CH_2), 1.43 (s, 9H, $(CH_3)_3$). MS m/z (ESI) 398.1 $[M+H]^+$.

4.1.6.5. (*R*)-1-(3-((2,6-dichloropyrido[3,4-*d*]pyrimidin-4-yl)amino)pyrrolidin-1-yl) prop-2-en-1-one (**22e**)

Light yellow solid. Yield 72.0%. ^{1}H NMR (400 MHz, $CDCl_3$) δ 8.97 (s, 1H, Ar-H), 8.12 (s, 1H, Ar-H), 7.61 (br, 1H, NH), 5.06–4.88 (m, 1H, CH), 3.77–3.48 (m, 1H, NCH_2), 2.38–2.12 (m, 2H, CH_2) 1.51 (s, 9H, $C(CH_3)_3$). MS m/z (ESI) 384.6 $[M+H]^+$.

4.1.6.6. (*S*)-1-(3-((2,6-dichloropyrido[3,4-*d*]pyrimidin-4-yl)amino)pyrrolidin-1-yl) prop-2-en-1-one (**22f**)

Light yellow solid. Yield 78.9%. ^{1}H NMR (400 MHz, $CDCl_3$) δ 8.94 (s, 1H, Ar-H), 8.18 (s, 1H, Ar-H), 7.84 (s, 1H, NH), 5.05–4.80 (m, 1H, CH), 3.75–3.48 (m,

4H, NCH_2), 2.39–2.11 (m, 2H, CH_2), 1.52 (s, 9H, $C(CH_3)_3$). MS m/z (ESI) 384.5 $[M+H]^+$.

4.1.6.7. (*R*)-1-(3-((2,6-dichloropyrido[3,4-*d*]pyrimidin-4-yl)amino)piperidin-1-yl) prop-2-en-1-one (**22g**)

Light yellow solid. Yield 89.5%. mp 110.5–112.5 °C. ^{1}H NMR (400 MHz, $CDCl_3$) δ 8.96 (s, 1H, Ar-H), 7.58 (s, 1H, Ar-H), 4.47–4.29 (m, 1H, NCH_2), 4.25–2.97 (m, 4H, NCH_2+CH), 2.46–1.45 (m, 13H, CH_2+$(CH_3)_3$). MS m/z (ESI) 398.6 $[M+H]^+$.

4.1.6.8. (*S*)-1-(3-((2,6-dichloropyrido[3,4-*d*]pyrimidin-4-yl)amino)piperidin-1-yl) prop-2-en-1-one (**22h**)

Light yellow solid. Yield 75.0%. mp 113.4–115.7 °C. ^{1}H NMR (400 MHz, $CDCl_3$) δ 8.96 (s, 1H, Ar-H), 7.58 (s, 1H, Ar-H), 4.46–4.27 (m, 1H, NCH_2), 4.24–2.99 (m, 4H, NCH_2+CH), 2.45–1.43 (m, 13H, CH_2+$(CH_3)_3$). MS m/z (ESI) 398.6 $[M+H]^+$.

4.1.7. Synthesis of intermediates **23a-h**

Intermediates **23a-h** was synthesized from intermediates **22a-h** with similar process to that of Intermediate **18**.

4.1.7.1. (*R*)-*N*-(1-(2,6-dichloropyrido[3,4-*d*]pyrimidin-4-yl)pyrrolidin-3-yl) acrylamide (**23a**)

Light yellow solid. Yield 46.0%. mp 206.5–208.7 °C. ^{1}H NMR (400 MHz, $CDCl_3$) δ 8.89 (s, 1H, Ar-H), 7.83 (s, 1H, Ar-H), 6.62 (d, *J* = 5.2 Hz, 1H, NH), 6.37 (dd, *J* = 16.9, 1.0 Hz, 1H, CH=CH_2), 6.18 (dd, *J* = 17.0, 10.3 Hz, 1H, CH=CH_2), 5.70 (dd, *J* = 10.3, 1.1 Hz, 1H, CH=CH_2), 4.89–4.68 (m, 1H, CH), 4.34–4.13 (m, 1H, NCH_2), 4.12–3.92 (m, 3H, NCH_2), 2.45–2.34 (m, 1H, CH_2), 2.34–2.17 (m, 1H, CH_2). MS m/z (ESI) 338.5 $[M+H]^+$.

4.1.7.2. (*S*)-*N*-(1-(2,6-dichloropyrido[3,4-*d*]pyrimidin-4-yl)pyrrolidin-3-yl) acrylamide (**23b**)

Light yellow solid. Yield 24.9%. mp 186.5–188.7 °C. ^{1}H NMR (400 MHz, $CDCl_3$) δ 8.89 (s, 1H, Ar-H), 7.83 (s, 1H, Ar-H), 6.68 (s, 1H, NH), 6.37 (dd, *J* = 17.0, 1.3 Hz, 1H, CH=CH_2), 6.18 (dd, *J* = 17.0, 10.3 Hz, 1H, CH=CH_2), 5.70 (dd, *J* = 10.3, 1.3 Hz, 1H, CH=CH_2), 4.80–4.75 (m, 1H, CH), 4.25–4.19 (m, 1H, NCH_2),4.05–3,98

(m, 3H, NCH_2), 2.44–2.33 (m, 1H, CH_2), 2.32–2.16 (m, 1H, CH_2). MS m/z (ESI) 338.4 $[M+H]^+$.

4.1.7.3. (*R*)-*N*-(1-(2,6-dichloropyrido[3,4-*d*]pyrimidin-4-yl)piperidin-3-yl)acrylamide (**23c**)

White solid. Yield 66.0%. mp 109.9–112.0 °C. ^{1}H NMR (400 MHz, $CDCl_3$) δ 9.03 (s, 1H, Ar-H), 7.91 (s, 1H, Ar-H), 6.41 (d, *J* = 5.2 Hz, 1H, NH), 6.33 (dd, *J* = 17.0, 1.1 Hz, 1H, $CH=CH_2$), 6.12 (dd, *J* = 17.0, 10.3 Hz, 1H, $CH=CH_2$), 5.70 (dd, *J* = 10.3, 1.1 Hz, 1H, $CH=CH_2$), 4.29–4.21 (m, 1H, CH), 4.15–4.06 (m, 2H, NCH_2), 3.81–3.71 (m, 2H, NCH_2), 2.09–2.03 (m, 1H, CH_2), 2.00–1.87 (m, 2H, CH_2), 1.85–1.77 (m, 1H, CH_2). MS m/z (ESI) 351.9 $[M+H]^+$.

4.1.7.4. (*S*)-*N*-(1-(2,6-dichloropyrido[3,4-*d*]pyrimidin-4-yl)piperidin-3-yl)acrylamide (**23d**)

White solid. Yield 79.2%. mp 113.0–114.8 °C. ^{1}H NMR (400 MHz, $CDCl_3$) δ 9.04 (s, 1H, Ar-H), 7.91 (s, 1H, Ar-H), 6.45 (s, 1H, NH), 6.33 (dd, *J* = 17.0, 1.2 Hz, 1H, $CH=CH_2$), 6.13 (dd, *J* = 17.0, 10.3 Hz, 1H, $CH=CH_2$), 5.69 (dd, *J* = 10.3, 1.2 Hz, 1H, $CH=CH_2$), 4.29–4.25 (m, 1H, CH), 4.13–4.09 (m, 2H, NCH_2), 3.84–3.78 (m, 2H, NCH_2), 2.08–2.00 (m, 1H, CH_2), 1.97–1.90 (m, 2H, CH_2), 1.88–1.80 (m, 1H, CH_2). MS m/z (ESI) 352.0 $[M+H]^+$.

4.1.7.5. (*R*)-1-(3-((2,6-dichloropyrido[3,4-*d*]pyrimidin-4-yl)amino)pyrrolidin-1-yl) prop-2-en-1-one (**23e**)

White solid. Yield 59.8%. ^{1}H NMR (400 MHz, DMSO-d_6) δ 9.06 (t, *J* = 5.3 Hz, 1H, NH), 8.89 (d, *J* = 2.1 Hz, 1H, Ar-H), 8.50 (d, *J* = 5.7 Hz, 1H, Ar-H), 6.73–6.52 (m, 1H, $CH=CH_2$), 6.26–6.10 (m, 1H, $CH=CH_2$), 5.79–5.65 (m, 1H, $CH=CH_2$), 4.86–4.62 (m, 1H, NH_2), 3.99–3.57 (m, 4H, NCH_2+CH), 2.33–2.01 (m, 2H, CH_2). mp 282.6–284.7 °C. MS m/z (ESI) 338.5 $[M+H]^+$.

4.1.7.6. (*S*)-1-(3-((2,6-dichloropyrido[3,4-*d*]pyrimidin-4-yl)amino)pyrrolidin-1-yl) prop-2-en-1-one (**23f**)

White solid. Yield 74.4%. mp 278.6–280.3 °C. ^{1}H NMR (400 MHz, DMSO-d_6) δ 9.08 (t, *J* = 5.6 Hz, 1H, NH), 8.90 (d, *J* = 2.0 Hz, 1H, Ar-H), 8.52 (d, *J* = 5.3 Hz, 1H, Ar-H), 6.75–6.52 (m, 1H, $CH=CH_2$), 6.29–6.08 (m, 1H, $CH=CH_2$), 5.75–5.65 (m, 1H,

$CH=CH_2$), 4.87–4.64 (m, 1H, NCH_2), 4.00–3.54 (m, 4H, NCH_2+CH), 2.36–2.00 (m, 2H, CH_2). MS m/z (ESI) 338.5 $[M+H]^+$.

4.1.7.7. *N*-((*3R*)-3-((2,6-dichloropyrido[3,4-*d*]pyrimidin-4-yl)amino)cyclohexyl) acrylamide (**23g**)

White solid. Yield 63.3%. ^{1}H NMR (400 MHz, DMSO-d_6) δ 9.01–8.74 (m, 2H, NH+Ar-H), 8.48 (d, *J* = 17.3 Hz, 1H, Ar-H), 6.89–6.77 (m, 1H, $CH=CH_2$), 6.17–6.06 (m, 1H, $CH=CH_2$), 5.73–5.63 (m, 1H, $CH=CH_2$), 4.59–4.13 (m, 1H, NCH_2), 4.07–3.87 (m, 1H, NCH_2), 3.14–3.01 (m, 1H, NCH_2), 2.92–2.70 (m, 1H, CH), 2.13–2.01 (m, 1H, CH_2), 1.92–1.47 (m, 3H, CH_2). MS m/z (ESI) 352.0$[M+H]^+$.

4.1.7.8. *N*-((*3R*)-3-((2,6-dichloropyrido[3,4-*d*]pyrimidin-4-yl)amino)cyclohexyl) acrylamide (**23h**)

White solid. Yield 68.8%. ^{1}H NMR (400 MHz, DMSO-d_6) δ 9.04–8.78 (m, 2H, NH+Ar-H), 8.48 (d, *J* = 16.4 Hz, 1H, Ar-H), 6.91–6.79 (m, 1H, $CH=CH_2$), 6.16–6.06 (m, 1H, $CH=CH_2$), 5.74–5.63 (m, 1H, $CH=CH_2$), 4.58–4.09 (m, 2H, NCH_2), 4.07–3.98 (m, 1H, NCH_2), 3.15–2.98 (m, 1H, NCH_2), 2.94–2.70 (m, 1H, CH), 2.21–1.99 (m, 1H, CH_2), 1.99–1.61 (m, 2H, CH_2), 1.62–1.43 (m, 1H, CH_2). mp 126.5–128.3 °C. MS m/z (ESI) 352.0 $[M+H]^+$.

4.1.8. General procedure for the synthesis of intermediates **24a-h**

To a mixture of intermediates **23a-h** (1 mmol) and *p*-toluenesulfonic acid (1.2 mmol) in 2-butyl alcohol (2-BuOH), aniline (1.1 mmol) was added. The mixture was refluxed for 1 h–2 h under nitrogen atmosphere. The solvent was removed under reduced pressure. The residue was suspended in $NaHCO_3$ solution and stirred at room temperature for 0.5 h. The yellow precipitate was collected and washed with water to give intermediates **24a-h**.

4.1.8.1. (*R*)-*N*-(1-(6-chloro-2-(phenylamino)pyrido[3,4-*d*]pyrimidin-4-yl)pyrrolidin -3-yl)acrylamide (**24a**)

Light yellow solid. Yield 100%. mp 120.2–122.8 °C. ^{1}H NMR (400 MHz, $CDCl_3$) δ 8.60 (s, 1H, Ar-H), 7.61 (d, *J* = 7.8 Hz, 2H, Ar-H), 7.58 (s, 1H, Ar-H), 7.31 (t, *J* = 7.9 Hz, 2H, Ar-H), 7.10 (s, 1H, NH), 7.04 (t, *J* = 7.4 Hz, 1H, Ar-H), 6.75 (s, NH), 6.40 (dd, *J* = 17.0, 1.4 Hz, 1H, $CH=CH_2$), 6.22 (dd, *J* = 16.9, 10.2 Hz, 1H, $CH=CH_2$), 5.71

(dd, *J* = 10.2, 1.4 Hz, 1H, $CH=CH_2$), 4.79–4.67 (m, 1H, CH), 4.09–4.01 (m, 1H, NCH_2), 3.99–3.87 (m, 2H, NCH_2), 3.84–3.77 (m, 1H, NCH_2), 2.34–2.19 (m, 2H, CH_2). MS m/z (ESI) 395.1 $[M+H]^+$.

4.1.8.2. (*S*)-*N*-(1-(6-chloro-2-(phenylamino)pyrido[3,4-*d*]pyrimidin-4-yl)pyrrolidin-3-yl)acrylamide (**24b**)

Light yellow solid. Yield 100%. mp 125.0–127.5 °C. ^{1}H NMR (400 MHz, $CDCl_3$) δ 8.59 (s, 1H, Ar-H), 7.60 (d, *J* = 7.9 Hz, 2H, Ar-H), 7.56 (d, *J* = 12.1 Hz, 1H, Ar-H), 7.30 (dd, *J* = 11.3, 4.5 Hz, 2H, Ar-H), 7.11 (s, 1H, NH), 7.03 (t, *J* = 7.4 Hz, 1H, Ar-H), 6.88 (s, 1H, NH), 6.40 (dd, *J* = 17.0, 1.4 Hz, 1H, $CH=CH_2$), 6.23 (dd, *J* = 16.8, 10.2 Hz, 1H, $CH=CH_2$), 5.71 (dd, *J* = 10.2 Hz, 1.4 Hz, 1H, $CH=CH_2$), 4.76–4.71 (m, 1H, CH), 4.06–3.78 (m, 4H, NCH_2), 2.35–2.20 (m, 2H, CH_2). MS m/z (ESI) 395.1 $[M+H]^+$.

4.1.8.3. (*R*)-*N*-(1-(6-chloro-2-(phenylamino)pyrido[3,4-*d*]pyrimidin-4-yl)piperidin-3-yl)acrylamide (**24c**)

Light yellow solid. Yield 76.1%. mp 203.3–205.5 °C. ^{1}H NMR (400 MHz, $CDCl_3$) δ 8.82 (s, 1H, Ar-H), 7.69 (d, *J* = 7.6 Hz, 2H, Ar-H), 7.63 (s, 1H, Ar-H), 7.35 (t, *J* = 7.4 Hz, 2H, Ar-H), 7.07 (t, *J* = 7.3 Hz, 1H, Ar-H), 6.37 (s, 1H, NH), 6.28 (dd, *J* = 17.0, 1.1 Hz, 1H, $CH=CH_2$), 5.99 (d, *J* = 17.0, 10.3 Hz, 1H, $CH=CH_2$), 5.62 (dd, *J* = 10.3, 1.1 Hz, 1H, $CH=CH_2$), 4.34–4.24 (m, 1H, CH), 3.97–3.90 (m, 1H, NCH_2), 3.86–3.77 (m, 1H, NCH_2), 3.75–3.64 (m, 2H, NCH_2), 2.06–1.98 (m, 1H, CH_2), 1.94–1.86 (m, 2H, CH_2), 1.83–1.77 (m, 1H, CH_2). MS m/z (ESI) 409.1 $[M+H]^+$.

4.1.8.4. (*S*)-*N*-(1-(6-chloro-2-(phenylamino)pyrido[3,4-*d*]pyrimidin-4-yl)piperidin-3-yl)acrylamide (**24d**)

Light yellow solid. Yield 64.4%. mp 197.2–199.3 °C. ^{1}H NMR (400 MHz, $CDCl_3$) δ 8.82 (s, 1H, Ar-H), 7.69 (d, *J* = 7.9 Hz, 2H, Ar-H), 7.65 (s, 1H, Ar-H), 7.35 (t, *J* = 7.9 Hz, 2H, Ar-H), 7.07 (t, *J* = 7.4 Hz, 1H, Ar-H), 6.34 (s, 1H, NH), 6.28 (dd, *J* = 16.9, 1.0 Hz, 1H, $CH=CH_2$), 5.99 (dd, *J* = 17.0, 10.3 Hz, 1H, $CH=CH_2$), 5.62 (d, *J* = 11.2 Hz, 1H, $CH=CH_2$), 4.32–4.26 (m, 1H, CH), 3.99–3.65 (m, 4H, NCH_2), 2.07–1.75 (m, 4H, CH_2). MS m/z (ESI) 409.1 $[M+H]^+$.

4.1.8.5. (*R*)-1-(3-((6-chloro-2-(phenylamino)pyrido[3,4-*d*]pyrimidin-4-yl)amino) pyrrolidin-1-yl)prop-2-en-1-one (**24e**)

Light yellow solid. Yield 88.6%. mp 151.5–154.0 °C. ^{1}H NMR (400 MHz, DMSO-d_6) δ 9.44 (s, 1H, NH), 8.62 (d, *J* = 2.8 Hz, 1H, Ar-H), 8.50–8.30 (m, 1H, NH), 8.29 (d, *J* = 7.4 Hz, 1H, Ar-H), 7.90 (d, *J* = 7.9 Hz, 2H, Ar-H), 7.30 (t, *J* = 7.9 Hz, 2H, Ar-H), 6.98–6.90 (m, 1H, Ar-H), 6.68–6.52 (m, 1H, $CH=CH_2$), 6.30–6.05 (m, 1H, $CH=CH_2$), 5.80–5.55 (m, 1H, $CH=CH_2$), 4.87–4.65 (m, 1H, CH), 3.90–3.44 (m, 4H, NCH_2), 2.35–2.05 (m, 2H, CH_2). MS m/z (ESI) 395.6 $[M+H]^+$.

4.1.8.6. (*S*)-1-(3-((6-chloro-2-(phenylamino)pyrido[3,4-*d*]pyrimidin-4-yl)amino) pyrrolidin-1-yl)prop-2-en-1-one (**24f**)

Light yellow solid. Yield 100%. mp 128.5–130.3 °C. ^{1}H NMR (400 MHz, DMSO-d_6) δ 9.46 (s, 1H, NH), 8.63 (d, *J* = 2.8 Hz, 1H, Ar-H), 8.51–8.34 (m, 1H, NH), 8.29 (d, *J* = 7.4 Hz, 1H, Ar-H), 7.91 (d, *J* = 7.9 Hz, 2H, Ar-H), 7.30 (t, *J* = 7.9 Hz, 2H, Ar-H), 6.99–6.92 (m, 1H, Ar-H), 6.70–6.54 (m, 1H, $CH=CH_2$), 6.28–6.07 (m, 1H, $CH=CH_2$), 5.78–5.57 (m, 1H, $CH=CH_2$), 4.89–4.67 (m, 1H, CH), 3.91–3.45 (m, 4H, NCH_2), 2.36–2.07 (m, 2H, CH_2). MS m/z (ESI) 395.6 $[M+H]^+$.

4.1.8.7. *N*-((*3R*)-3-((6-chloro-2-(phenylamino)pyrido[3,4-*d*]pyrimidin-4-yl)amino) cyclohexyl)acrylamide (**24g**)

Light yellow solid. Yield 96.9%. mp 117.1–119.2 °C. ^{1}H NMR (400 MHz, DMSO-d_6) δ 9.42 (s, 1H, NH), 8.62 (s, 1H, Ar-H), 8.29–8.15 (m, 2H, Ar-H+NH), 7.86 (d, *J* = 7.6 Hz, 2H, Ar-H), 7.26 (t, *J* = 6.3 Hz, 2H, Ar-H), 7.03–6.97 (m, 1H, Ar-H), 6.57–6.51 (m, 1H, $CH=CH_2$), 6.25–5.94 (m, 1H, $CH=CH_2$), 5.81–5.46 (m, 1H, $CH=CH_2$), 4.57–4.01 (m, 3H, NCH_2), 3.32–2.75 (m, 2H, NCH_2+NH), 2.14–2.03 (m, 1H, CH_2), 1.92–1.43 (m, 3H, CH_2). MS m/z (ESI) 409.0 $[M+H]^+$.

4.1.8.8. *N*-((3*S*)-3-((6-chloro-2-(phenylamino)pyrido[3,4-*d*]pyrimidin-4-yl)amino) cyclohexyl)acrylamide (**24h**)

Light yellow solid. Yield 86.7%. mp 118.0–120.3 °C. ^{1}H NMR (400 MHz, DMSO-d_6) δ 9.40 (s, 1H, NH), 8.62 (s, 1H, Ar-H), 8.27–8.12 (m, 2H, Ar-H+NH), 7.86 (d, *J* = 7.6 Hz, 2H, Ar-H), 7.26 (t, *J* = 6.3 Hz, 2H, Ar-H), 7.01–6.95 (m, 1H, Ar-H), 6.59–6.51 (m, 1H, $CH=CH_2$), 6.27–5.97 (m, 1H, $CH=CH_2$), 5.80–5.45 (m, 1H,

$CH=CH_2$), 4.60–4.00 (m, 3H, NCH_2), 3.30–2.79 (m, 2H, NCH_2+NH), 2.15–2.02 (m, 1H, CH_2), 1.94–1.42 (m, 3H, CH_2). MS m/z (ESI) 409.0 $[M+H]^+$.

4.1.9. 2,6-Dichloro-4-(pyrrolidin-1-yl)pyrido[3,4-*d*]pyrimidine (**26**)

Intermediate **26** was synthesized from intermediate **21** and tetrahydropyrrol with similar process to that of intermediates **22a-h**. Light yellow solid. Yield 91.0%. mp 246.8–249.5 °C. ^1H NMR (400 Mz, $CDCl_3$) δ 8.98 (s, 1H, Ar-H), 7.94 (s, 1H, Ar-H), 3.98 (s, 4H, NCH_2), 2.13 (s, 4H, CH_2). MS m/z (ESI) 233.7 $[M+H]^+$.

4.1.10. Synthesis of intermediates **27a** and **27b**

Intermediates **27a** and **27b** was synthesized from intermediate **26** with similar operations to that of intermediates **24a-h**.

4.1.10.1. 6-Chloro-*N*-phenyl-4-(pyrrolidin-1-yl)pyrido[3,4-*d*]pyrimidin-2-amine (**27a**)

Light yellow solid. Yield 99.2%. mp 270.8–272.8 °C. ^1H NMR (400 MHz, $CDCl_3$) δ 8.75 (s, 1H, Ar-H), 7.80 (s, 1H, Ar-H), 7.70 (d, J = 7.7 Hz, 2H, Ar-H), 7.34 (t, J = 8.0 Hz, 2H, Ar-H), 7.16 (s, 1H, NH), 7.04 (t, J = 7.4 Hz, 1H, Ar-H), 3.91 (s, 4H, NCH_2), 2.09 (t, J = 6.5 Hz, 4H, CH_2). MS m/z (ESI) 326.0 $[M+H]^+$.

4.1.10.2. 6-Chloro-*N*-(3-fluorophenyl)-4-(pyrrolidin-1-yl)pyrido[3,4-*d*]pyrimidin-2-amine (**27b**)

Light yellow solid. Yield 91.8%. mp 232.7–234.8 °C. ^1H NMR (400 MHz, $CDCl_3$) δ 8.76 (s, 1H, Ar-H), 7.86–7.81 (m, 1H, Ar-H), 7.81 (s, 1H, Ar-H), 7.28–7.17 (m, 4H, Ar-H), 6.76–6.67 (m, 1H, Ar-H), 3.96–3.88 (s, 4H, NCH_2), 2.13–2.08 (m, 4H, CH_2). MS m/z (ESI) 344.5 $[M+H]^+$.

4.1.11. Synthesis of intermediates **27c-g**

Sodium hydride (NaH, 60%, 3 mmol) was added to a solution of alcohol (1.1 mmol) in dried THF. The mixture was stirred at room temperature for 0.5 h. Then intermediate **26** (1 mmol) was added and the mixture was stirred at room temperature for another 2 h, concentrated under reduced pressure. The residue was suspended in water. The precipitate was collected, washed with water and dried to give intermediates **27c-g**.

4.1.11.1. 6-Chloro-4-(pyrrolidin-1-yl)-2-((tetrahydro-2*H*-pyran-4-yl)oxy)pyrido[3,4-*d*]pyrimidine (**27c**)

Light yellow solid. Yield 100%. mp 130.5–132.9 °C. ^{1}H NMR (400 MHz, $CDCl_3$) δ 8.80 (s, 1H, Ar-H), 7.87 (s, 1H, Ar-H), 5.36–5.23 (m, 1H, CH), 4.08–4.00 (m, 2H, OCH_2), 3.98–3.89 (m, 4H, NCH_2), 3.64–3.56 (m, 2H, OCH_2), 2.16–2.11 (m, 2H, CH_2), 2.10–2.06 (m, 4H, CH_2), 1.96–1.87 (m, 2H, CH_2). MS m/z (ESI) 335.0 $[M+H]^+$.

4.1.11.2. 2-(Benzyloxy)-6-chloro-4-(pyrrolidin-1-yl)pyrido[3,4-*d*]pyrimidine (**27d**)

Light yellow solid. Yield 99.0%. mp 161.8–163.5 °C. ^{1}H NMR (400 MHz, $CDCl_3$) δ 8.83 (s, 1H, ArH), 7.87 (s, 1H, ArH), 7.50 (d, *J* = 7.2 Hz, 2H, ArH), 7.37–7.27 (m, 3H, ArH), 5.48 (s, 2H, OCH_2), 3.96–3.89 (m, 4H, NCH_2), 2.11–2.05 (m, 4H, CH_2). MS m/z (ESI) 341.1 $[M+H]^+$.

4.1.11.3. 6-Chloro-2-((4-fluorobenzyl)oxy)-4-(pyrrolidin-1-yl)pyrido[3,4-*d*] pyrimidine (**27e**)

Light yellow solid. Yield 90.0%. mp 212.0–215.2 °C. ^{1}H NMR (400 MHz, $CDCl_3$) δ 8.83 (s, 1H, Ar-H), 7.87 (s, 1H, Ar-H), 7.48 (dd, *J* = 8.5, 5.5 Hz, 2H, Ar-H), 7.02 (dd, *J* = 12.1, 5.3 Hz, 2H, Ar-H), 5.44 (s, 2H, OCH_2), 3.99–3.85 (m, 4H, NCH_2), 2.14–2.01 (m, 4H, CH_2). MS m/z (ESI) 359.1 $[M+H]^+$.

4.1.11.4. 6-Chloro-4-(pyrrolidin-1-yl)-2-((tetrahydro-2*H*-pyran-4-yl)methoxy)pyrido [3,4-*d*]pyrimidine (**27f**)

Light yellow solid. Yield 98.0%. mp 250.0–251.7 °C. ^{1}H NMR (400 MHz, $CDCl_3$) δ 8.82 (s, 1H, Ar-H), 7.87 (s, 1H, Ar-H), 4.26 (d, *J* = 6.9 Hz, 2H, $OC\underline{H}_2CH$), 4.03–3.97 (m, 2H, OCH_2), 3.98–3.86 (m, 4H, NCH_2), 3.49–3.37 (m, 2H, OCH_2), 2.21–2.12 (m, 1H, $OCH_2C\underline{H}$), 2.12–2.02 (m, 4H, CH_2), 1.83–1.76 (m, 2H, CH_2), 1.50–1.39 (m, 2H, CH_2). MS m/z (ESI) 349.2 $[M+H]^+$.

4.1.11.5. 6-Chloro-2-(cyclohexylmethoxy)-4-(pyrrolidin-1-yl)pyrido[3,4-*d*] pyrimidine (**27g**)

Light yellow solid. Yield 98.0%. mp 146.9–149.6 °C. ^{1}H NMR (400 MHz, $CDCl_3$) δ 8.82 (s, 1H, Ar-H), 7.86 (s, 1H, Ar-H), 4.21 (d, *J* = 6.3 Hz, 2H, OCH_2), 3.97–3.89 (m, 4H, NCH_2), 2.13–2.04 (m, 4H, NCH_2), 1.91–1.86 (m, 2H, CH_2), 1.80–1.71 (m, 2H, CH_2), 1.70–1.65 (m, 1H, CH), 1.29–1.22 (m, 4H, CH_2), 1.09–1.00

(m, 2H, CH_2). MS m/z (ESI) 347.1 $[M+H]^+$.

4.1.12. Synthesis of intermediate **28**

2,6-Diaminopyridine was used to prepare *N*-(6-aminopyridin-2-yl)acrylamide (**28**).[49]

4.1.13. General procedure for the synthesis of title compounds **20a-d**, **25a-h** and **29a-g**

The mixture of intermediate **18** (or **24a-h** or **27a-g**, 0.50 mmol), intermediate **19** (or **28**, 0.55 mmol), $Pd(OAc)_2$ (0.05 mmol), X-phos (or Xantphos, 0.15 mmol), Cs_2CO_3 (1.25 mmol) and 1,4-dioxane (or 1,2-dimethoxyethane, DME) were refluxed under argon atmosphere for 1 h–4 h. The solvent was removed under reduced pressure and the residue was purified by silica gel column chromatography to produce title compounds **20a-d**, **25a-h** and **29a-g**.

4.1.13.1. (*R*)-*N*-(1-(6-((2-methoxy-4-(2-methoxyethoxy)phenyl)amino)pyrido[3,4-*d*] pyrimidin-4-yl)pyrrolidin-3-yl)acrylamide (**20a**)

Light yellow solid. Yield 46.3%. mp 167.5–169.4 °C. ^{1}H NMR (400 MHz, DMSO-d_6) δ 8.71 (s, 1H, Ar-H), 8.54 (d, *J* = 6.5 Hz, 1H, NH), 8.30 (s, 1H, NH), 8.28 (s, 1H, Ar-H), 7.74 (d, *J* = 8.7 Hz, 1H, Ar-H), 7.41 (s, 1H, Ar-H), 6.66 (d, *J* = 2.0 Hz, 1H, Ar-H), 6.51 (dd, *J* = 8.7, 2.0 Hz, 1H, $CH=CH_2$), 6.30–6.09 (m, 1H, Ar-H+$CH=CH_2$), 5.68–5.54 (m, 1H, $CH=CH_2$), 4.52–4.43 (m, *J* = 3.9 Hz, 1H, NCH_2), 4.10–4.07 (m, 2H, OCH_2), 3.99–3.87 (m, 2H, NCH_2), 3.83 (s, 3H, Ar-OCH_3), 3.78–3.72 (m, 1H, NCH_2), 3.69–3.64 (m, 2H, OCH_2), 3.63–3.54 (m, 1H, NCH_2), 3.33 (s, 3H, OCH_3), 2.25–1.96 (m, 2H, CH_2). ^{13}C NMR (100 MHz, DMSO-d_6) δ 165.0, 157.8, 155.1, 153.8, 152.1, 151.9, 149.8, 139.2, 131.9, 126.0, 123.6, 123.0, 122.5, 105.1, 100.0, 99.7, 71.0, 67.5, 58.6, 56.1, 55.8, 53.8, 48.8, 42.0.MS m/z (ESI) 465.9$[M+H]^+$.

4.1.13.2. (*R*)-*N*-(1-(6-((4-(2-(dimethylamino)ethoxy)-2-methoxyphenyl)amino) pyrido[3,4-*d*]pyrimidin-4-yl)pyrrolidin-3-yl)acrylamide (**20b**)

Light yellow solid. Yield 35.7%. mp 236.9–238.4 °C. ^{1}H NMR (400 MHz, $CDCl_3$) δ 8.94 (s, 1H, Ar-H), 8.47 (s, 1H, Ar-H), 7.55 (d, *J* = 8.6 Hz, 1H, Ar-H), 7.41–7.28 (m, 3H, Ar-H+$CH=CH_2$), 6.71 (s, 1H, Ar-H), 6.63 (d, *J* = 2.5 Hz, 1H,

$CH=CH_2$), 6.54 (dd, J = 8.6, 2.5 Hz, 1H, $CH=CH_2$), 4.43–4.29 (m, 2H, OCH_2), 3.88 (s, 3H, OCH_3), 3.19–3.09 (m, 2H, NCH_2), 2.68 (s, 6H, $N(CH_3)_2$). MS m/z (ESI) 479.0 $[M+H]^+$.

4.1.13.3. (*R*)-*N*-(1-(6-((2-methoxy-4-(4-methylpiperazin-1-yl)phenyl)amino)pyrido[3,4-*d*]pyrimidin-4-yl)pyrrolidin-3-yl)acrylamide (**20c**)

Light yellow solid. Yield 38.6%. mp 297.9–300.1 °C. ^{1}H NMR (400 MHz, DMSO-d_6) δ 8.73 (s, 1H, NH), 8.59–8.43 (m, 2H, Ar-H+NH), 8.40 (s, 1H, Ar-H), 7.79 (d, J = 8.7 Hz, 1H, Ar-H), 7.54 (s, 1H, Ar-H), 6.73 (d, J = 2.2 Hz, 1H, Ar-H), 6.55 (dd, J = 8.8, 2.2 Hz, 1H, Ar-H), 6.33–5.99 (m, 2H, $CH=CH_2$), 5.64 (dd, J = 9.8, 2.4 Hz, 1H, $CH=CH_2$), 4.56–4.46 (m, 1H, NCH_2), 4.30–3.70 (m, 10H, OCH_3+NCH_2), 3.60–3.47 (m, 2H, NCH_2), 3.26–3.13 (m, 2H, NCH_2), 2.99–2.92 (m, 1H, CH), 2.88 (s, 3H), 2.30–2.18 (m, 1H, CH_2), 2.10–1.96 (m, 1H, CH_2). ^{13}C NMR (100 MHz, DMSO-d_6) δ 165.1, 158.0, 154.5, 151.4, 150.3, 146.5, 146.4, 131.8, 126.2, 123.1, 122.5, 122.1, 108.0, 101.5, 101.1, 63.4, 56.4, 56.1, 52.7 (C×2), 49.6, 46.8 (C×2), 42.5, 41.9. MS m/z (ESI) 490.0 $[M+H]^+$.

4.1.13.4. (*R*)-*N*-(1-(6-((5-(4-methylpiperazin-1-yl)pyridin-2-yl)amino)pyrido[3,4-*d*]pyrimidin-4-yl)pyrrolidin-3-yl)acrylamide (**20d**)

Light yellow solid. Yield 35.6%. mp 292.5–297.5 °C. ^{1}H NMR (400 MHz, DMSO-d_6) δ 9.78 (s, 1H, NH), 9.12 (s, 1H, Ar-H), 8.81 (s, 1H, Ar-H), 8.57 (d, J = 6.4 Hz, 1H, Ar-H), 8.37 (s, 1H, Ar-H), 7.98 (d, J = 2.8 Hz, 1H, Ar-H), 7.47 (dd, J = 9.1, 2.9 Hz, 1H, Ar-H), 7.27 (d, J = 9.0 Hz, 1H, Ar-H), 6.27 (dd, J = 17.1, 10.0 Hz, 1H, $CH=CH_2$), 6.14 (dd, J = 17.1, 2.3 Hz, 1H, $CH=CH_2$), 5.64 (dd, J = 10.0, 2.3 Hz, 1H, $CH=CH_2$), 4.60–4.49 (m, 1H, CH), 4.41–4.17 (m, 1H, NCH_2), 4.14–3.94 (m, 2H, NCH_2), 3.93–3.84 (m, 1H, NCH_2), 3.32–3.17 (m, 4H, NCH_2), 3.15–2.94 (m, 4H, NCH_2), 2.62 (s, 3H, NCH_3), 2.32–2.19 (m, 1H, CH_2), 2.11–1.96 (m, 1H, CH_2). MS m/z (ESI) 460.4 $[M+H]^+$.

4.1.13.5. (*R*)-*N*-(1-(6-((5-(4-methylpiperazin-1-yl)pyridin-2-yl)amino)-2-(phenylamino)pyrido[3,4-*d*]pyrimidin-4-yl)pyrrolidin-3-yl)acrylamide (**25a)**

Light yellow solid. Yield 62.4%. mp 243.5–247.0 °C. ^{1}H NMR (400 MHz, DMSO-d_6) δ 9.47 (s, 1H, NH), 9.05 (s, 1H, Ar-H), 9.02 (s, 1H, Ar-H), 8.58 (s, 1H, NH), 8.55 (d, J = 6.7 Hz, 1H, Ar-H), 7.91 (m, 3H, Ar-H), 7.42 (dd, J = 9.1, 2.9 Hz, 1H,

Ar-H), 7.24 (m, 3H, NH+Ar-H), 6.88 (t, *J* = 7.3 Hz, 1H, Ar-H), 6.27 (dd, *J* = 17.1, 10.0 Hz, 1H, CH=CH_2), 6.14 (dd, *J* = 17.1, 2.3 Hz, 1H, CH=CH_2), 5.64 (dd, *J* = 10.0, 2.3 Hz, 1H, CH=CH_2), 4.62–4.48 (m, 1H, CH), 4.37–4.18 (m, 1H, NCH_2), 4.17–3.96 (m, 2H, NCH_2), 3.94–3.85 (m, 1H, NCH_2), 3.19–3.07 (m, 4H, NCH_2), 2.79–2.62 (m, 4H, NCH_2), 2.39 (s, 3H, NCH_3), 2.31–2.22 (m, 1H, CH_2), 2.14–2.00 (m, 1H, CH_2). ^{13}C NMR (100 MHz, DMSO-d_6) δ 165.1, 159.2, 155.8, 149.0, 148.2, 147.5, 142.7, 142.0, 141.0, 134.7, 131.9, 128.8 (Ar-C×2), 127.7, 126.0, 120.7, 118.9, 118.8 (Ar-C×2), 112.2, 102.9, 56.0, 54.7 (C×2), 49.2 (C×2), 48.9, 45.8. HRMS m/z (ESI): calcd for $C_{29}H_{37}FN_9O$ $[M+H]^+$ 551.29898, found 551.29895.

4.1.13.6. (*S*)-*N*-(1-(6-((5-(4-methylpiperazin-1-yl)pyridin-2-yl)amino)-2-(phenylamino)pyrido[3,4-*d*]pyrimidin-4-yl)pyrrolidin-3-yl)acrylamide (**25b)**

Light yellow solid. Yield 54.0%. mp 246.5–250.5 °C. ^{1}H NMR (400 MHz, DMSO-d_6) δ 9.46 (s, 1H, NH), 9.04 (s, 1H, Ar-H), 9.02 (s, 1H, Ar-H), 8.58 (s, 1H, NH), 8.54 (d, *J* = 6.7 Hz, 1H, Ar-H), 7.92 (s, 1H, NH), 7.90 (s, 1H, Ar-H), 7.41 (dd, *J* = 9.0, 2.8 Hz, 1H, Ar-H), 7.26 (t, *J* = 7.8 Hz, 2H, Ar-H), 7.21 (d, *J* = 9.0 Hz, 1H, Ar-H), 6.88 (t, *J* = 7.3 Hz, 1H, Ar-H), 6.26 (dd, *J* = 17.1, 10.0 Hz, 1H, CH=CH_2), 6.15 (dd, *J* = 17.1, 2.3 Hz, 1H, CH=CH_2), 5.64 (dd, *J* = 10.0, 2.2 Hz, 1H, CH=CH_2), 4.64–4.45 (m, 1H, CH), 4.42–4.18 (m, 1H, NCH_2), 4.19–3.95 (m, 2H, NCH_2), 3.95–3.80 (m, 1H, NCH_2), 3.15–3.01 (m, 4H, NCH_2), 2.67–2.53 (s, 4H, NCH_2), 2.32 (s, 3H, NCH_3), 2.30–2.23 (m, 1H, CH_2), 2.15–1.97 (m, 1H, CH_2). ^{13}C NMR (100 MHz, DMSO-d_6) δ 165.1, 159.2, 155.8, 149.0, 148.2, 147.5, 142.7, 142.0, 141.0, 134.7, 131.9, 128.8 (Ar-C×2), 127.7, 126.0, 120.8, 118.9, 118.8 (Ar-C×2), 112.2, 102.7, 56.0, 54.7 (C×2), 49.2 (C×2), 48.9, 45.8. HRMS m/z (ESI): calcd for $C_{29}H_{37}FN_9O$ $[M+H]^+$ 551.29898, found 551.29895.

4.1.13.7. (*R*)-*N*-(1-(6-((5-(4-methylpiperazin-1-yl)pyridin-2-yl)amino)-2-(phenylamino)pyrido[3,4-*d*]pyrimidin-4-yl)piperidin-3-yl)acrylamide (**25c)**

Light yellow solid. Yield 40.4%. mp 194.8–196.7 °C. ^{1}H NMR (400 MHz, DMSO-d_6) δ 9.51 (s, 1H, NH), 9.22 (s, 1H, NH), 8.67 (s, 1H, Ar-H), 8.63 (s, 1H, Ar-H), 8.27 (d, *J* = 7.6 Hz, 1H, CONH), 7.92 (d, *J* = 7.9 Hz, 2H, Ar-H), 7.88 (d, *J* = 2.9 Hz, 1H, Ar-H), 7.40 (dd, *J* = 9.1, 3.0 Hz, 1H, Ar-H), 7.27 (t, *J* = 7.9 Hz, 2H, Ar-H), 7.15 (d, *J* = 9.1 Hz, 1H, Ar-H), 6.91 (t, *J* = 7.3 Hz, 1H, Ar-H), 6.26 (dd, *J* = 17.1, 10.1 Hz, 1H, CH=CH_2), 6.11 (dd, *J* = 17.1, 2.2 Hz, 1H, CH=CH_2), 5.61 (dd, *J* = 10.1, 2.2

Hz, 1H, $CH=CH_2$), 4.38–4.28 (m, 1H, NCH_2), 4.25–4.17 (m, 1H, NCH_2), 4.09–4.00 (m, 1H, NCH_2), 3.27–3.21 (m, 1H, NCH_2), 3.16–3.10 (m, 1H, CH), 3.08 (s, 4H, NCH_2), 2.52 (s, 4H, NCH_2), 2.27 (s, 3H, NCH_3), 2.13–1.97 (m, 2H, CH_2), 1.91–1.86 (m, 1H, CH_2), 1.64–1.52 (m, 1H, CH_2). ^{13}C NMR (100 MHz, DMSO-d_6) δ 172.5, 164.6, 163.7, 155.3, 148.8, 148.5, 148.2, 142.9, 141.7, 141.3, 134.6, 132.1, 128.8 (Ar-C×2), 127.6, 125.9, 121.1, 118.9 (Ar-C×2), 112.3, 101.8, 54.9 (C×2), 53.2, 50.0, 49.3 (C×2), 46.3, 46.0, 30.9, 23.9. HRMS m/z (ESI): calcd for $C_{29}H_{37}FN_9O$ $[M+H]^+$ 565.31463, found 565.31537.

4.1.13.8. (*S*)-*N*-(1-(6-((5-(4-methylpiperazin-1-yl)pyridin-2-yl)amino)-2-(phenylamino)pyrido[3,4-*d*]pyrimidin-4-yl)piperidin-3-yl)acrylamide (**25d)**

Light yellow solid. Yield 67.7%. mp 197.0–200.0 °C. ^{1}H NMR (400 MHz, DMSO-d_6) δ 9.51 (s, 1H, NH), 9.22 (s, 1H, NH), 8.67 (s, 1H, Ar-H), 8.63 (s, 1H, Ar-H), 8.27 (d, *J* = 7.6 Hz, 1H, CONH), 7.92 (d, *J* = 7.9 Hz, 2H, Ar-H), 7.88 (d, *J* = 2.9 Hz, 1H, Ar-H), 7.40 (dd, *J* = 9.1, 3.0 Hz, 1H, Ar-H), 7.27 (t, *J* = 7.9 Hz, 2H, Ar-H), 7.15 (d, *J* = 9.1 Hz, 1H, Ar-H), 6.91 (t, *J* = 7.3 Hz, 1H, Ar-H), 6.26 (dd, *J* = 17.1, 10.1 Hz, 1H, $CH=CH_2$), 6.11 (dd, *J* = 17.1, 2.2 Hz, 1H, $CH=CH_2$), 5.61 (dd, *J* = 10.1, 2.2 Hz, 1H, $CH=CH_2$), 4.44–4.26 (m, 1H, NCH_2), 4.26–4.14 (m, 1H, NCH_2), 4.10–3.96 (m, 1H, NCH_2), 3.28–3.22 (m, 1H, NCH_2), 3.14–3.10 (m, 1H, CH), 3.10–3.04 (m, 4H, NCH_2), 2.52 (s, 4H, NCH_2), 2.27 (s, 3H, NCH_3), 2.14–1.98 (m, 2H, CH_2), 1.91–1.86 (m, 1H, CH_2), 1.65–1.50 (m, 1H, CH_2). ^{13}C NMR (100 MHz, DMSO-d_6) δ 172.5, 164.6, 163.7, 155.3, 148.8, 148.5, 148.2, 142.9, 141.7, 141.3, 134.6, 132.1, 128.8 (Ar-C×2), 127.6, 125.9, 121.1, 118.9 (Ar-C×2), 112.3, 101.8, 54.9 (C×2), 53.2, 50.0, 49.3 (C×2), 46.3, 46.0, 30.8, 23.9. HRMS m/z (ESI): calcd for $C_{29}H_{37}FN_9O$ $[M+H]^+$ 565.31463, found 565.31537.

4.1.13.9. (*R*)-1-(3-((6-((5-(4-methylpiperazin-1-yl)pyridin-2-yl)amino)-2-(phenyl amino)pyrido[3,4-*d*]pyrimidin-4-yl)amino)pyrrolidin-1-yl)prop-2-en-1-one (**25e)**

Light yellow solid. Yield 42.1%. mp 175.3–176.9 °C. ^{1}H NMR (400 MHz, DMSO-d_6) δ 9.24 (d, *J* = 9.4 Hz, 1H, NH), 9.11 (s, 1H, NH), 8.58 (s, 1H, Ar-H), 8.28 (s, 1H, Ar-H), 8.19 (dd, *J* = 14.5, 6.0 Hz, 1H, Ar-H), 7.97–7.88 (m, 3H, Ar-H), 7.40 (d, *J* = 9.0 Hz, 1H, Ar-H), 7.27 (t, *J* = 7.8 Hz, 2H, Ar-H), 7.15 (d, *J* = 9.1 Hz, 1H, Ar-H), 6.90 (t, *J* = 7.3 Hz, 1H, Ar-H), 6.70–6.55 (m, 1H, $CH=CH_2$), 6.22–6.12 (m, 1H, $CH=CH_2$), 5.73–5.60 (m, 1H, $CH=CH_2$), 4.91–4.70 (m, 1H, CH), 3.98–3.79 (m, 1H,

NCH_2), 3.73–3.63 (m, 1H, NCH_2), 3.60–3.45 (m, 2H, NCH_2), 3.18–3.02 (m, 4H, NCH_2), 2.62–2.48 (m, 4H, NCH_2), 2.42–2.29 (m, 1H, CH_2), 2.27 (s, 3H, NCH_3), 2.23–2.12 (m, 1H, CH_2). HRMS m/z (ESI): calcd for $C_{29}H_{37}FN_9O$ $[M+H]^+$ 551.29898, found 551.29895. $[\alpha]_D^{20}$ –22.9° (c 2.1, MeOH).

4.1.13.10. (*S*)-1-(3-((6-((5-(4-methylpiperazin-1-yl)pyridin-2-yl)amino)-2-(phenyl amino)pyrido[3,4-*d*]pyrimidin-4-yl)amino)pyrrolidin-1-yl)prop-2-en-1-one (**25f)**

Light yellow solid. Yield 23.7%. mp 160.4–162.5 °C. ^{1}H NMR (400 MHz, DMSO-d_6) δ 9.24 (d, *J* = 9.4 Hz, 1H, NH), 9.11 (s, 1H, NH), 8.58 (s, 1H, Ar-H), 8.28 (s, 1H, Ar-H), 8.19 (dd, *J* = 14.5, 6.0 Hz, 1H, Ar-H), 7.97–7.88 (m, 3H, Ar-H), 7.40 (d, *J* = 9.0 Hz, 1H, Ar-H), 7.27 (t, *J* = 7.8 Hz, 2H, Ar-H), 7.15 (d, *J* = 9.1 Hz, 1H, Ar-H), 6.90 (t, *J* = 7.3 Hz, 1H, Ar-H), 6.71–6.56 (m, 1H, $CH=CH_2$), 6.23–6.13 (m, 1H, $CH=CH_2$), 5.74–5.62 (m, 1H, $CH=CH_2$), 4.90–4.69 (m, 1H, CH), 3.97–3.79 (m, 1H, NCH_2), 3.72–3.64 (m, 1H, NCH_2), 3.59–3.44 (m, 2H, NCH_2), 3.08 (s, 4H, NCH_2), 2.52 (s, 4H, NCH_2), 2.42–2.29 (m, 1H, CH_2), 2.27 (s, 3H, NCH_3), 2.23–2.12 (m, 1H, CH_2). MS m/z (ESI) 551.3 $[M+H]^+$.

4.1.13.11. (*R*)-1-(3-((6-((5-(4-methylpiperazin-1-yl)pyridin-2-yl)amino)-2-(phenyl amino)pyrido[3,4-*d*]pyrimidin-4-yl)amino)piperidin-1-yl)prop-2-en-1-one (**25g)**

Light yellow solid. Yield 44.4%. mp 146.8–148.5 °C. ^{1}H NMR (400 MHz, DMSO-d_6) δ 9.26 (s, 1H, NH), 9.04 (d, *J* = 7.3 Hz, 1H, NH), 8.56 (s, 1H, Ar-H), 8.29 (s, 1H, Ar-H), 7.96–7.86 (m, 4H, Ar-H), 7.41 (dd, *J* = 9.0, 2.9 Hz, 1H, Ar-H), 7.24 (t, *J* = 7.4 Hz, 2H, Ar-H), 7.14 (d, *J* = 9.0 Hz, 1H, Ar-H), 6.94–6.73 (m, 2H, Ar-H+$CH=CH_2$), 6.21–6.03 (m, 1H, $CH=CH_2$), 5.77–5.55 (m, 1H, $CH=CH_2$), 4.56–4.25 (m, 2H, NCH_2), 4.20–3.98 (m, 1H, NCH_2), 3.31–3.22 (m, 1H, NCH_2), 3.10–3.05 (m, 4H, NCH_2), 2.97–2.78 (m, 1H, CH), 2.50–2.46 (m, 4H, NCH_2), 2.25 (s, 3H, NCH_3), 2.13–2.04 (m, 1H, CH_2), 1.88–1.75 (m, 2H, CH_2), 1.54–1.43 (m, 1H, CH_2). ^{13}C NMR (100 MHz, DMSO-d_6) δ 165.1, 158.8, 158.7, 156.0, 148.7, 147.6, 141.9, 141.4, 134.9, 129.0, 128.8 (Ar-C×2), 127.9, 127.6, 127.5, 120.9, 119.0 (Ar-C×2), 118.4, 112.1, 100.3, 55.0 (C×2), 49.5 (C×2), 48.2, 47.3, 46.2, 42.2, 30.1, 25.5. MS m/z (ESI) 565.4 $[M+H]^+$.

4.1.13.12. (*S*)-1-(3-((6-((5-(4-methylpiperazin-1-yl)pyridin-2-yl)amino)-2-(phenyl amino)pyrido[3,4-*d*]pyrimidin-4-yl)amino)piperidin-1-yl)prop-2-en-1-one (**25h)**

Light yellow solid. Yield 40.4%. mp 125.3–127.1 °C. ^{1}H NMR (400 MHz, DMSO-d_6) δ 9.27 (s, 1H, NH), 9.04 (d, J = 7.0 Hz, 1H, NH), 8.57 (s, 1H, Ar-H), 8.29 (s, 1H, Ar-H), 8.04–7.81 (m, 4H, Ar-H), 7.41 (dd, J = 9.0, 2.9 Hz, 1H, Ar-H), 7.24 (t, J = 7.3 Hz, 2H, Ar-H), 7.14 (d, J = 9.0 Hz, 1H, Ar-H), 6.97–6.70 (m, 2H, Ar-H), 6.28–5.95 (m, 1H, $CH=CH_2$), 5.87–5.48 (m, 1H, $CH=CH_2$), 4.54–4.27 (m, 2H, NCH_2), 4.19–3.98 (m, 1H, NCH_2), 3.31–3.23 (m, 1H, NCH_2), 3.09 (s, 4H, NCH_2), 2.97–2.78 (m, 1H, CH), 2.53 (s, 4H, NCH_2), 2.27 (s, 3H, NCH_3), 2.15–2.02 (m, 1H, CH_2), 1.89–1.74 (m, 2H, CH_2), 1.59–1.43 (m, 1H, CH_2). ^{13}C NMR (100 MHz, DMSO-d_6) δ 165.1, 158.8, 158.9, 156.0, 148.7, 147.6, 141.9, 141.5, 134.9, 129.0, 128.8 (Ar-C×2), 127.9, 127.6, 127.6, 120.9, 118.9 (Ar-C×2), 118.3, 112.1, 100.3, 55.1 (C×2), 49.6 (C×2), 48.2, 47.3, 46.3, 45.9, 30.1, 25.5. HRMS m/z (ESI): calcd for $C_{29}H_{37}FN_9O$ $[M+H]^+$ 565.31463, found 565.31537. $[\alpha]_D^{20}$ +5.8° (c 2.0, MeOH).

4.1.13.13. *N*-(6-((2-(phenylamino)-4-(pyrrolidin-1-yl)pyrido[3,4-*d*]pyrimidin-6-yl) amino)pyridin-2-yl)acrylamide (**29a)**

Light yellow solid. Yield 24.0%. mp 212.5–214.5 °C. ^{1}H NMR (400 MHz, DMSO-d_6) δ 10.12 (s, 1H, NH), 9.64 (s, 1H, NH), 9.04 (s, 1H, Ar-H), 8.87 (s, 1H, Ar-H), 8.60 (s, 1H, NH), 7.91 (d, J = 8.0 Hz, 2H, Ar-H), 7.63 (t, J = 7.9 Hz, 1H, Ar-H), 7.53 (d, J = 7.8 Hz, 1H, Ar-H), 7.26 (t, J = 7.8 Hz, 2H, Ar-H), 6.94 (d, J = 8.1 Hz, 2H, Ar-H), 6.88 (t, J = 7.2 Hz, 1H, Ar-H), 6.64 (dd, J = 17.0, 10.2 Hz, 1H, $CH=CH_2$), 6.33 (d, J = 16.9 Hz, 1H, $CH=CH_2$), 5.81 (d, J = 11.5 Hz, 1H, $CH=CH_2$), 4.18–3.82 (m, 4H, NCH_2), 2.07–1.90 (m, 4H, CH_2). ^{13}C NMR (100 MHz, DMSO-d_6) δ 163.8, 158.9, 156.2, 154.1, 149.8, 147.6, 147.0, 143.6, 142.0, 139.6, 132.1, 128.8 (Ar-C×2), 128.0, 120.8, 118.8 (Ar-C×2), 118.7, 107.8, 105.4, 104.3, 50.7 (C×2). MS m/z (ESI) 453.1 $[M+H]^+$.

4.1.13.14. *N*-(6-((2-((3-fluorophenyl)amino)-4-(pyrrolidin-1-yl)pyrido[3,4-*d*] pyrimidin-6-yl)amino)pyridin-2-yl)acrylamide (**29b)**

Light yellow solid. Yield 22.7%. mp 196.5–198.0 °C. ^{1}H NMR (400 MHz, DMSO-d_6) δ 10.13 (s, 1H, NH), 9.68 (s, 1H, NH), 9.33 (s, 1H, Ar-H), 8.89 (s, 1H, Ar-H), 8.63 (s, 1H, Ar-H), 8.03 (d, J = 12.9 Hz, 1H, Ar-H), 7.64 (t, J = 8.0 Hz, 1H, Ar-H), 7.58 (d, J = 8.3 Hz, 1H, Ar-H), 7.54 (d, J = 7.8 Hz, 1H, Ar-H), 7.26 (dd, J = 15.5, 8.1 Hz, 1H, Ar-H), 6.94 (d, J = 8.0 Hz, 1H, Ar-H), 6.66 (m, 2H, Ar-H+ $CH=CH_2$), 6.33 (dd, J = 17.0, 1.8 Hz, 1H, $CH=CH_2$), 5.82 (dd, J = 10.2, 1.8 Hz, 1H,

CH=CH_2), 4.18–3.90 (m, 4H, NCH_2), 2.05 –1.95 (m, 4H, CH_2). ^{13}C NMR (100 MHz, DMSO-d_6) δ 163.81, 162.9 (d, J_{C-F} = 237 Hz), 158.9, 155.9, 154.1, 149.8, 147.8, 147.3, 143.9 (d, J_{C-F} = 12 Hz), 143.2, 139.6, 132.0, 130.2 (d, J_{C-F} = 10 Hz), 128.0, 118.9, 114.5 (d, J_{C-F} = 1.7 Hz), 114.5, 107.8, 106.8 (d, J_{C-F} = 21 Hz), 105.4(d, J_{C-F} = 20 Hz) , 105.0, 104.2, 50.8 (C×2). MS m/z (ESI) 471.3 $[M+H]^+$.

4.1.13.15. *N*-(6-((4-(pyrrolidin-1-yl)-2-((tetrahydro-2H-pyran-4-yl)oxy)pyrido[3,4-*d*] pyrimidin-6-yl)amino)pyridin-2-yl)acrylamide (**29c)**

Light yellow solid. Yield 41.9%. mp 198.5–200.5 °C. ^{1}H NMR (400 MHz, DMSO-d_6) δ 10.13 (s, 1H, NH), 9.72 (s, 1H, NH), 8.92 (s, 1H, Ar-H), 8.63 (s, 1H, Ar-H), 7.65 (t, *J* = 8.0 Hz, 1H, Ar-H), 7.54 (d, *J* = 7.8 Hz, 1H, Ar-H), 6.97 (t, *J* = 11.4 Hz, 1H, Ar-H), 6.63 (dd, *J* = 17.0, 10.2 Hz, 1H, CH=CH_2), 6.33 (dd, *J* = 17.0, 1.6 Hz, 1H, CH=CH_2), 5.81 (dd, *J* = 11.5 Hz, 1.6 Hz, 1H, CH=CH_2), 5.22–5.13 (m, 1H, OCH), 4.37–3.61 (m, 6H, NCH_2+OCH_2), 3.60–3.42 (m, 2H, CH_2), 2.09–2.00 (m, 2H, CH_2), 1.98–1.86 (s, 4H, CH_2), 1.72–1.60 (m, 2H, CH_2). ^{13}C NMR (100 MHz, DMSO-d_6) δ 163.8, 160.6, 160.4, 154.0, 149.8, 148.1 (Ar-C×2), 143.0, 139.7, 132.0, 128.0, 119.7, 107.9, 105.6, 103.9, 70.6, 65.4(C×2), 50.8 (C×2), 32.5 (C×2). MS m/z (ESI) 462.9 $[M+H]^+$.

4.1.13.16. *N*-(6-((2-(benzyloxy)-4-(pyrrolidin-1-yl)pyrido[3,4-*d*]pyrimidin-6-yl) amino)pyridin-2-yl)acrylamide (**29d)**

Light yellow solid. Yield 21.0%. mp 224.0–226.0 °C. ^{1}H NMR (400 MHz, DMSO-d_6) δ 10.13 (s, 1H, NH), 9.74 (s, 1H, NH), 8.93 (s, 1H, Ar-H), 8.67 (s, 1H, Ar-H), 7.65 (t, *J* = 8.0 Hz, 1H, Ar-H), 7.55 (d, *J* = 7.8 Hz, 1H, Ar-H), 7.49 (d, *J* = 7.1 Hz, 2H, Ar-H), 7.40 (t, *J* = 7.3 Hz, 2H, Ar-H), 7.33 (m, 1H, Ar-H), 6.96 (d, *J* = 8.0 Hz, 1H, Ar-H), 6.63 (dd, *J* = 17.0, 10.2 Hz, 1H, CH=CH_2), 6.33 (dd, *J* = 17.0, 1.8 Hz, 1H, CH=CH_2), 5.81 (dd, *J* = 10.2, 1.8 Hz, 1H, CH=CH_2), 5.39 (s, 2H, OCH_2), 3.96 (br, 4H, NCH_2), 2.03–1.96 (m, 4H, CH_2). ^{13}C NMR (100 MHz, DMSO-d_6) δ 163.8, 161.2, 160.3, 154.0, 149.8, 148.2, 148.2, 142.8, 139.7, 137.9, 132.0, 128.8 (Ar-C×2), 128.5 (Ar-C×2), 128.2, 128.1, 119.9, 107.9, 105.7, 104.1, 67.9, 50.8 (C×2). MS m/z (ESI) 468.1 $[M+H]^+$.

4.1.13.17. *N*-(6-((2-((4-fluorobenzyl)oxy)-4-(pyrrolidin-1-yl)pyrido[3,4-*d*]pyrimidin-6-yl)amino)pyridin-2-yl)acrylamide (**29e)**

Light yellow solid. Yield 26.6%. mp 224.5–227.0 °C. ^{1}H NMR (400 MHz, DMSO-d_6) δ 10.14 (s, 1H, NH), 9.75 (s, 1H, NH), 8.94 (s, 1H, Ar-H), 8.67 (s, 1H, Ar-H), 7.65 (t, J = 8.0 Hz, 1H, Ar-H), 7.55 (m, 3H, Ar-H), 7.22 (t, J = 8.8 Hz, 2H, Ar-H), 6.96 (d, J = 8.1 Hz, 1H, Ar-H), 6.62 (dd, J = 17.0, 10.2 Hz, 1H, $CH=CH_2$), 6.33 (dd, J = 17.0, 1.7 Hz, 1H, $CH=CH_2$), 5.81 (d, J = 11.5 Hz, 1H, $CH=CH_2$), 5.37 (s, 2H, OCH_2), 3.96 (br, 4H, NCH_2), 2.03–1.96 (s, 4H, CH_2). ^{13}C NMR (100 MHz, DMSO-d_6) δ 163.8, 162.2 (d, J_{C-F} = 240 Hz), 161.2, 160.3, 153.9, 149.8, 148.3, 148.2, 134.1 (d, J_{C-F} = 2 Hz), 132.0, 130.9 (d, J_{C-F} = 8 Hz, Ar-C×2), 128.1, 119.9, 115.6 (d, J_{C-F} = 22 Hz, Ar-C×2), 107.9, 105.7, 104.0, 67.2, 50.8 (C×2). MS m/z (ESI) 486.9 $[M+H]^+$.

4.1.13.18. *N*-(6-((4-(pyrrolidin-1-yl)-2-((tetrahydro-2H-pyran-4-yl)methoxy)pyrido [3,4-*d*]pyrimidin-6-yl)amino)pyridin-2-yl)acrylamide (**29f)**

Light yellow solid. Yield 27.6%. mp 236.0–238.5 °C. ^{1}H NMR (400 MHz, DMSO-d_6) δ 10.14 (s, 1H, NH), 9.72 (s, 1H, NH), 8.92 (s, 1H, Ar-H), 8.64 (s, 1H, Ar-H), 7.65 (t, J = 8.0 Hz, 1H, Ar-H), 7.54 (d, J = 7.8 Hz, 1H, Ar-H), 6.96 (d, J = 8.1 Hz, 1H, Ar-H), 6.63 (dd, J = 17.0, 10.2 Hz, 1H, $CH=CH_2$), 6.33 (dd, J = 17.0, 1.7 Hz, 1H, $CH=CH_2$), 5.81 (dd, J = 10.2, 1.8 Hz, 1H, $CH=CH_2$), 4.15 (d, J = 6.6 Hz, 2H, OCH_2), 4.01 (br, 4H, NCH_2), 3.94–3.86 (m, 2H, OCH_2), 3.37 (s, 1H, OCH_2), 3.31 (s, 1H, OCH_2), 2.05–1.98 (m, 1H, CH), 1.98–1.93 (m, 4H, CH_2), 1.71–1.65 (m, 2H, CH_2), 1.36–1.30 (m, 2H, CH_2). ^{13}C NMR (100 MHz, DMSO-d_6) δ 163.8, 161.5, 160.2, 154.0, 149.8, 148.1 (Ar-C×2), 142.9, 139.6, 132.0, 128.0, 119.7, 107.9, 105.6, 104.0, 71.0, 67.1 (C×2), 50.8(C×2), 34.8, 29.9 (C×2). MS m/z (ESI) 477.0 $[M+H]^+$.

4.1.13.19. *N*-(6-((2-(cyclohexylmethoxy)-4-(pyrrolidin-1-yl)pyrido[3,4-*d*]pyrimidin-6-yl)amino)pyridin-2-yl)acrylamide (**29g)**

Light yellow solid. Yield 17.6%. mp 234.0–236.5 °C. ^{1}H NMR (400 MHz, DMSO-d_6) δ 10.13 (s, 1H, NH), 9.71 (s, 1H, NH), 8.91 (s, 1H, Ar-H), 8.63 (s, 1H, Ar-H), 7.64 (t, J = 8.0 Hz, 1H, Ar-H), 7.54 (d, J = 7.8 Hz, 1H, Ar-H), 6.97 (t, J = 10.3 Hz, 1H, Ar-H), 6.63 (dd, J = 17.0, 10.1 Hz, 1H, $CH=CH_2$), 6.33 (d, J = 15.7 Hz, 1H, $CH=CH_2$), 5.81 (d, J = 11.5 Hz, 1H, $CH=CH_2$), 4.10 (d, J = 6.3 Hz, 2H, OCH_2), 4.63–3.50 (s, 4H, NCH_2), 2.08–1.89 (s, 4H, CH_2), 1.82–1.66 (m, 5H, $CH+CH_2$), 1.34–1.09 (m, 4H, CH_2), 1.09–0.99 (m, 2H, CH_2). ^{13}C NMR (100 MHz, DMSO-d_6) δ 163.8, 161.6, 160.2, 154.0, 149.8, 148.1, 148.0, 142.9, 139.6, 132.0, 128.0, 119.7,

107.9, 105.6, 104.0, 71.6, 50.8(C×2), 37.4, 29.9(C×2), 26.5, 25.8 (C×2). MS m/z (ESI) 474.1 $[M+H]^+$.

4.2. Biology

4.2.1. Cell culture

The three selected human lung cancer cell lines HCC827, H1975 and A549 were grown as a monolayer respectively. The three cell lines were maintained in RPMI-1640 medium supplemented with 10% heat inactivated fetal bovine serum (FBS). Additional 1% sodium pyruvate 100 mM solution was added when culture HCC827 cells. All cancer cells were incubated in a humidified atmosphere containing 5% CO_2 at 37 °C.

4.2.2. MTT assay

Cellular chemosensitivity was determined by using a modified 3-[4,5-dimethylthiazol-2-yl]-2,5-diphenyl-*2H*-tetrazolium bromide (MTT) colorimetric assay *in vitro*. HCC827, H1975 or A549 cells in 200 μL culture medium were seeded into 96-well plates at 3000-5000 cells per well and cultured in RPMI 1640 10% FBS, incubated at 37 °C for 24 h prior to drug exposure. Cells were treated with final concentrations of 0.33, 1, 33, 100, 333, 1000, 3333, 10000 nM of tested compounds simultaneously and incubated for 72 h and then 20 μL of MTT solution (5 mg/mL in PBS) was added to each well and incubated for 4 h. The culture medium was removed carefully and the formed blue formazan crystals were dissolved in 150 μL DMSO. The optical density at 490 nm was determined by Varioskan Flash Multimode Reader (Thermo scientific). At least three separate experiments with triplicate data were performed to obtain mean cell viability. The IC_{50} value, that is, the concentration (μM) of a compound was able to cause 50% cell death with respect to the control culture, was calculated according to the inhibition ratios.

4.2.3. *In vitro* enzymatic activity assay

Theses assays were carried out as described by Kashem.[50] All of the enzymatic reactions were conducted at 30 °C for 40 minutes. The 50 μL reaction mixture contains 40 mM Tris, pH 7.4, 10 mM $MgCl_2$, 0.1 mg/mL BSA, 1 mM DTT, 10 μM ATP, 25 ng kinase and the 0.2 mg/ml enzyme substrate (Poly (Glu, Tyr)). The compounds were diluted in 10% DMSO and 5 μL of the dilution was added to a 50

μL reaction so that the final concentration of DMSO is 1% in all of reactions. The assay was performed by using Kinase-Glo Plus luminescence kinase assay kit. It measures kinase activity by quantitating the amount of ATP remaining in solution following a kinase reaction. The luminescent signal from the assay is correlated with the amount of ATP present and is inversely correlated with the amount of kinase activity.

The percentage of inhibition was calculated based on the following equation:

% inhibition rate = $[1-(Lu_{compound}-Lu_{min})/(Lu_{max}-Lu_{min})]\times100\%$,

Where $Lu_{compound}$ is the signal at a given compound concentration, Lu_{max} is the signal of EGFRs without compound and Lu_{min} is the signal of background in the absence of enzyme and compound. The IC_{50} values were calculated using nonlinear regression with normalized dose-response fit using GraphPad Prism 5.0 Software.

4.2.4. Western blot assay

HCC827 and H1975 cells were seeded in 6-well plates at 1×10^6 per well, incubated at 37 °C with 5% CO_2 for 24 h before drug exposure. Cells were treated with different concentrations of **25h** or osimertinib for 8 h, then collected and suspended in lysis buffer (Beyotime) and centrifuged for 20 minutes at 12000 rpm, later removed the insoluble material. Same amounts of proteins were loaded and separated by 8% SDS-PAGE and transferred to polyvinylidene fluoride membranes (Millpore) after that. The anti-EGFR, anti-pEGFR (Tyr1068) and anti-ERK were diluted at 1:1000, while the anti-pERK (Thr202/Tyr204) was diluted at 1:2000. All antibodies above were purchased from Cell Signaling Technology. Anti-GAPDH was diluted at 1:2000 and the secondary antibodies were used at 1:10000. The results were detected by an enhanced chemiluminescene system (Millpore).

4.2.5. Cell apoptosis assay

HCC827 cells were plated in 12-well plates , incubated at 37 °C with 5% CO_2 for 16 h. Fresh growth medium with **25h** or AZD9291 (3 μM) was added. Medium with 0.03% DMSO was used as control. After incubating for another 24 h, growth medium was collected and cells were trypsined and collected correspondingly to the medium. The cells were disposed using an Annexin V-FITC apoptosis detection kit according to the instructions and apoptosis rate was determined under the Flow Cytometry.

4.2.6. *In vivo* antitumor effect on established HCC827 xenograft model

BALB/c nude mice (4-week old, female) were purchased from Beijing Vital River Laboratory Animal Technology Co., Ltd. and fed at Xi'an Jiaotong University Health Science Center for 2 weeks. The experimental protocol was approved by Ethic Committee of Xi'an Jiaotong University.

HCC827 cells were harvested during the exponential growth phase, washed three times with PBS, and resuspended at a concentration of 1×10^7–1.5×10^7 cells/mL. Tumor xenograft models were established by subcutaneously injecting 200 μL of tumor cell suspension into the right flank of mice (6 weeks old). The mice were randomized into three groups (5-6 mice per group) prior to treatment with compound **25h**. The animals were given compound **25h** (10 mg/kg and 50 mg/kg) and vehicle alone (10% NMP plus 50% PEG400 in sterile water) once daily via oral gavage. Tumors were measured every three days using calipers, and their volume was calculated using the following formula: tumor volume = $a\times b^2\times0.5$ (a = long diameter; b = short diameter).

The tumor growth inhibition (TGI, %) was calculated based on the following equation:

$$\%\ TGI = [1-(V_{d21,\ 25h} - V_{d0,\ 25h})/(V_{d21,\ vehicle} - V_{d0,\ vehicle})]\times100\%,$$

$V_{d21,\ 25h}$ and $V_{d0,\ 25h}$ are mean tumor volume of **25h** group on d21and d0, respectively; $V_{d21,\ vehicle}$ and $V_{d0,\ vehicle}$ are mean tumor volume of vehicle group on d21; and d0, respectively.

4.3. Molecule docking

The protein-ligand complex crystal structure of AEE788[8] with $EGFR^{T790M}$ was chosen as the template to elucidate the binding mode of compounds **20d**, **25a** and **25h**. Protein structure (PDB 2JIU) was downloaded from Protein Data Bank and the Sybyl-X 2.0 software was used for molecular docking. The EGFR was defined as a receptor after the preparation of adding hydrogen atoms and deleting waters. The site sphere was selected on the basis of the ligand binding location of AEE788, which was replaced by our compounds. After end of molecular docking, 20 docking poses were scored and selected based on total score. The images of binding mode were prepared by applying PyMol 1.6 software.

4.4. Statistical analysis

The data are reported as mean in kinase activity assay for at least two experiments and mean ± standard deviation (SD) in cell antiproliferation assay. Statistical differences were analyzed according to one way ANOVA test wherein the differences were considered to be significant at $p < 0.05$. All statistics were calculated using the statistical program Graph Pad Prism 5.0 software.

Acknowledgments

Financial support from The National Natural Science Foundation of China (Grant No. 81673354) is gratefully acknowledged.

References

1. M.A. Olayioye, R.M. Neve, H.A. Lane, N.E. Hynes**.** *EMBO J.* **2000**, *19*, 3159.
2. M.M. Moasser**.** *Oncogene* **2007**, *26*, 6577.
3. C.E. Geyer, J. Forster, D. Lindquist, S. Chan, C.G. Romieu, T. Pienkowski, A. Jagiello-Gruszfeld, J. Crown, A. Chan, B. Kaufman, D. Skarlos, M. Campone, N. Davidson, M. Berger, C. Oliva, S.D. Rubin, S. Stein, D. Cameron. *N. Engl. J. Med.* **2006**, *355*, 2733.
4. T.S. Mok, Y.-L. Wu, S. Thongprasert, C.-H. Yang, D.-T. Chu, N. Saijo, P. Sunpaweravong, B. Han, B. Margono, Y. Ichinose, Y. Nishiwaki, Y. Ohe, J.-J. Yang, B. Chewaskulyong, H. Jiang, E.L. Duffield, C.L. Watkins, A.A. Armour, M. Fukuoka**.** *N. Engl. J. Med.* **2009**, *361*, 947.
5. F.A. Shepherd, J.R. Pereira, T. Ciuleanu, E.H. Tan, V. Hirsh, S. Thongprasert, D. Campos, S. Maoleekoonpiroj, M. Smylie, R. Martins, M. van Kooten, M. Dediu, B. Findlay, D.S. Tu, D. Johnston, A. Bezjak, G. Clark, P. Santabarbara, L. Seymour, T. Natl Canc Inst Canada Clin**.** *N. Engl. J. Med.* **2005**, *353*, 123.
6. K.D. Carey, A.J. Garton, M.S. Romero, J. Kahler, S. Thomson, S. Ross, F. Park, J.D. Haley, N. Gibson, M.X. Sliwkowski**.** *Cancer Res.* **2006**, *66*, 8163.
7. S. Kobayashi, T.J. Boggon, T. Dayaram, P.A. Jänne, O. Kocher, M. Meyerson, B.E. Johnson, M.J. Eck , D.G. Tenen , B. Halmos. *N. Engl. J. Med.* **2005**, *352*, 786.
8. A. Asadujjaman, V. Ahmadi, M. Yalcin, N. ten Brummelhuis, A. Bertin**.** *Polym. Chem.* **2017**, *8*, 3140.
9. J. Engel, J. Lategahn, D. Rauh**.** *ACS Med. Chem. Lett.* **2016**, *7*, 2.
10. K.-H. Yin, Y.-H. Hsieh, R.S. Sulake, S.-P. Wang, J.-I. Chao, C. Chen**.** *Bioorg. Med. Chem. Lett.* **2014**, *24*, 5247.
11. S.-N. Li, Y.-Y. Xu, J.-Y. Gao, H.-r. Yin, S.-L. Zhang, H.-Q. Li**.** *Bioorg. Med. Chem.* **2015**, *23*, 3221.
12. M.M. Hamed, E.E.D.A. Abou, A.B. Keeton, G.A. Piazza, A.H. Abadi, R.W. Hartmann, M.

Engel**.** *ChemMedChem* **2013**, *8*, 1495.

13. S.-J. Zuo, S. Zhang, S. Mao, X.-X. Xie, X. Xiao, M.-H. Xin, W. Xuan, Y.-Y. He, Y.-X. Cao, S.-Q. Zhang**.** *Bioorg. Med. Chem.* **2016**, *24*, 179.
14. D. Li, L. Ambrogio, T. Shimamura, S. Kubo, M. Takahashi, L.R. Chirieac, R.F. Padera, G.I. Shapiro, A. Baum, F. Himmelsbach, W.J. Rettig, M. Meyerson, F. Solca, H. Greulich, K.K. Wong**.** *Oncogene* **2008**, *27*, 4702.
15. J.A. Engelman, K. Zejnullahu, C.M. Gale, E. Lifshits, A.J. Gonzales, T. Shimamura, F. Zhao, P.W. Vincent, G.N. Naumov, J.E. Bradner, I.W. Althaus, L. Gandhi, G.I. Shapiro, J.M. Nelson, J.V. Heymach, M. Meyerson, K.K. Wong, P.A. Janne**.** *Cancer Res.* **2007**, *67*, 11924.
16. S.K. Rabindran, C.M. Discafani, E.C. Rosfjord, M. Baxter, M.B. Floyd, J. Golas, W.A. Hallett, B.D. Johnson, R. Nilakantan, E. Overbeek, M.F. Reich, R. Shen, X. Shi, H.R. Tsou, Y.F. Wang, A. Wissner**.** *Cancer Res.* **2004**, *64*, 3958.
17. Y. Kim, J. Ko, Z. Cui, A. Abolhoda, J.S. Ahn, S.H. Ou, M.J. Ahn, K. Park**.** *Mol. Cancer Ther.* **2012**, *11*, 784.
18. M.L. Sos, H.B. Rode, S. Heynck, M. Peifer, F. Fischer, S. Klueter, V.G. Pawar, C. Reuter, J.M. Heuckmann, J. Weiss, L. Ruddigkeit, M. Rabiller, M. Koker, J.R. Simard, M. Getlik, Y. Yuza, T.-H. Chen, H. Greulich, R.K. Thomas, D. Rauh**.** *Cancer Res.* **2010**, *70*, 868.
19. D.A.E. Cross, S.E. Ashton, S. Ghiorghiu, C. Eberlein, C.A. Nebhan, P.J. Spitzler, J.P. Orme, M.R.V. Finlay, R.A. Ward, M.J. Mellor, G. Hughes, A. Rahi, V.N. Jacobs, M.R. Brewer, E. Ichihara, J. Sun, H. Jin, P. Ballard, K. Al-Kadhimi, R. Rowlinson, T. Klinowska, G.H.P. Richmond, M. Cantarini, D.-W. Kim, M.R. Ranson, W. Pao**.** *Cancer Discov.* **2014**, *4*, 1046.
20. M.R.V. Finlay, M. Anderton, S. Ashton, P. Ballard, P.A. Bethel, M.R. Box, R.H. Bradbury, S.J. Brown, S. Butterworth, A. Campbell, C. Chorley, N. Colclough, D.A.E. Cross, G.S. Currie, M. Grist, L. Hassall, G.B. Hill, D. James, M. James, P. Kemmitt, T. Klinowska, G. Lamont, S.G. Lamont, N. Martin, H.L. McFarland, M.J. Mellor, J.P. Orme, D. Perkins, P. Perkins, G. Richmond, P. Smith, R.A. Ward, M.J. Waring, D. Whittaker, S. Wells, G.L. Wrigley**.** *J. Med. Chem.* **2014**, *57*, 8249.
21. P.A. Jaenne, J.C.-H. Yang, D.-W. Kim, D. Planchard, Y. Ohe, S.S. Ramalingam, M.-J. Ahn, S.-W. Kim, W.-C. Su, L. Horn, D. Haggstrom, E. Felip, J.-H. Kim, P. Frewer, M. Cantarini, K.H. Brown, P.A. Dickinson, S. Ghiorghiu, M. Ranson**.** *N. Engl. J. Med.* **2015**, *372*, 1689.
22. Z. Piotrowska, M.J. Niederst, C.A. Karlovich, H.A. Wakelee, J.W. Neal, M. Mino-Kenudson, L. Fulton, A.N. Hata, E.L. Lockerman, A. Kalsy, S. Digumarthy, A. Muzikansky, M. Raponi, A.R. Garcia, H.E. Mulvey, M.K. Parks, R.H. DiCecca, D. Dias-Santagata, A.J. Iafrate, A.T. Shaw, A.R. Allen, J.A. Engelman, L.V. Sequist**.** *Cancer Discov.* **2015**, *5*, 713.
23. S. Wang, S. Cang, D. Liu**.** *J. Hematol. Oncol.* **2016**, *9*, 34.
24. X. Xu, L. Mao, W. Xu, W. Tang, X. Zhang, B. Xi, R. Xu, X. Fang, J. Liu, C. Fang, L. Zhao, X. Wang, J. Jiang, P. Hu, H. Zhao, L. Zhang**.** *Mol. Cancer Ther.* **2016**, *15*, 2586.
25. S. Planken, D.C. Behenna, S.K. Nair, T.O. Johnson, A. Nagata, C. Almaden, S. Bailey, T.E.

Ballard, L. Bernier, H. Cheng, S. Cho-Schultz, D. Dalvie, J.G. Deal, D.M. Dinh, M.P. Edwards, R.A. Ferre, K.S. Gajiwala, M. Hemkens, R.S. Kania, J.C. Kath, J. Matthews, B.W. Murray, S. Niessen, S.T. Orr, M. Pairish, N.W. Sach, H. Shen, M. Shi, J. Solowiej, K. Tran, E. Tseng, P. Vicini, Y. Wang, S.L. Weinrich, R. Zhou, M. Zientek, L. Liu, Y. Luo, S. Xin, C. Zhang, J. Lafontaine**.** *J. Med. Chem.* **2017**, *60*, 3002.

26. H. Cheng, S.K. Nair, B.W. Murray, C. Almaden, S. Bailey, S. Baxi, D. Behenna, S. Cho-Schultz, D. Dalvie, D.M. Dinh, M.P. Edwards, J.L. Feng, R.A. Ferre, K.S. Gajiwala, M.D. Hemkens, A. Jackson-Fisher, M. Jalaie, T.O. Johnson, R.S. Kania, S. Kephart, J. Lafontaine, B. Lunney, K.K. Liu, Z. Liu, J. Matthews, A. Nagata, S. Niessen, M.A. Ornelas, S.T. Orr, M. Pairish, S. Planken, S. Ren, D. Richter, K. Ryan, N. Sach, H. Shen, T. Smeal, J. Solowiej, S. Sutton, K. Tran, E. Tseng, W. Vernier, M. Walls, S. Wang, S.L. Weinrich, S. Xin, H. Xu, M.J. Yin, M. Zientek, R. Zhou, J.C. Kath**.** *J. Med. Chem.* **2016**, *59*, 2005.
27. Z. Song, Y. Ge, C. Wang, S. Huang, X. Shu, K. Liu, Y. Zhou, X. Ma**.** *J. Med. Chem.* **2016**, *59*, 6580.
28. L. Chen, W. Fu, L. Zheng, Z. Liu, G. Liang**.** *J. Med. Chem.* **2017**. DOI: 10.1021/acs.jmedchem.7b01310.
29. H. Patel, R. Pawara, A. Ansari, S. Surana**.** *Eur. J. Med. Chem.* **2017**, *142*, 32.
30. L. Yu, M. Huang, T. Xu, L. Tong, X.-e. Yan, Z. Zhang, Y. Xu, C. Yun, H. Xie, K. Ding, X. Lu**.** *Eur. J. Med. Chem.* **2017**, *126*, 1107.
31. X. Lu, L. Yu, Z. Zhang, X. Ren, J.B. Smaill, K. Ding**.** *Med. Res. Rev.* **2018**. DOI: 10.1002/med.21488.
32. J. Engel, C. Becker, J. Lategahn, M. Keul, J. Ketzer, T. Muhlenberg, L. Kollipara, C. Schultz-Fademrecht, R.P. Zahedi, S. Bauer, D. Rauh**.** *Angew. Chem.-Int. Edit.* **2016**, *55*, 10909.
33. J. Engel, S. Smith, J. Lategahn, H.L. Tumbrink, L. Goebel, C. Becker, E. Hennes, M. Keul, A. Unger, H. Muller, M. Baumann, C. Schultz-Fademrecht, G. Gunther, J.G. Hengstler, D. Rauh**.** *J. Med. Chem.* **2017**, *60*, 7725.
34. M. Gunther, M. Juchum, G. Kelter, H. Fiebig, S. Laufer**.** *Angew. Chem.-Int. Edit.* **2016**, *55*, 10890.
35. M. Juchum, M. Gunther, E. Doring, A. Sievers-Engler, M. Lammerhofer, S. Laufer**.** *J. Med. Chem.* **2017**, *60*, 4636.
36. M. Gunther, J. Lategahn, M. Juchum, E. Doring, M. Keul, J. Engel, H.L. Tumbrink, D. Rauh, S. Laufer**.** *J. Med. Chem.* **2017**, *60*, 5613.
37. H. Park, H.Y. Jung, S. Mah, S. Hong**.** *Angew. Chem.-Int. Edit.* **2017**, *56*, 7634.
38. H. Zhang, J. Wang, Y. Shen, H.Y. Wang, W.M. Duan, H.Y. Zhao, Y.Y. Hei, M. Xin, Y.X. Cao, S.Q. Zhang**.** *Eur. J. Med. Chem.* **2018**, *148*, 221.
39. Y.-Y. Hei, Y. Shen, J. Wang, H. Zhang, H.-Y. Zhao, M. Xin, Y.-X. Cao, Y. Li, S.-Q. Zhang**.** *Bioorg. Med. Chem.* **2018**, 26, 2173

40. F. Lovering, J. Bikker, C. Humblet**.** *J. Med. Chem.* **2009**, *52*, 6752.
41. G.A. Nishiguchi, A. Rico, H. Tanner, R.J. Aversa, B.R. Taft, S. Subramanian, L. Setti, M.T. Burger, L. Wan, V. Tamez, A. Smith, Y. Lou, P.A. Barsanti, B.A. Appleton, M. Mamo, L. Tandeske, I. Dix, J.E. Tellew, S. Huang, L.A. Mathews Griner, V.G. Cooke, A. Van Abbema, H. Merritt, S. Ma, K. Gampa, F. Feng, J. Yuan, Y. Wang, J.R. Haling, S. Vaziri, M. Hekmat-Nejad, J.M. Jansen, V. Polyakov, R. Zang, V. Sethuraman, P. Amiri, M. Singh, E. Lees, W. Shao, D.D. Stuart, M.P. Dillon, S. Ramurthy**.** *J. Med. Chem.* **2017**, *60*, 4869.
42. M. Ishikawa, Y. Hashimoto**.** *J. Med. Chem.* **2011**, *54*, 1539.
43. S. Xu, T. Xu, L. Zhang, Z. Zhang, J. Luo, Y. Liu, X. Lu, Z. Tu, X. Ren, K. Ding**.** *J. Med. Chem.* **2013**, *56*, 8803.
44. Y. Hao, X. Wang, T. Zhang, D. Sun, Y. Tong, Y. Xu, H. Chen, L. Tong, L. Zhu, Z. Zhao, Z. Chen, J. Ding, H. Xie, Y. Xu, H. Li**.** *J. Med. Chem.* **2016**, *59*, 7111.
45. W. Zhou, X. Liu, Z. Tu, L. Zhang, K. Xin, F. Bai, Z. Zhao, Y. Xu, K. Ding, H. Li**.** *J. Med. Chem.* **2013**, *56*, 7821.
46. Z. Song, S. Huang, H. Yu, Y. Jiang, C. Wang, Q. Meng, X. Shu, H. Sun, K. Liu, Y. Li, X. Ma**.** *Eur. J. Med. Chem.* **2017**, *133*, 329.
47. C.-H. Yun, K.E. Mengwasser, A.V. Toms, M.S. Woo, H. Greulich, K.-K. Wong, M. Meyerson, M.J. Eck**.** *Proc. Natl. Acad. Sci. U. S. A.* **2008**, *105*, 2070.
48. T. Nakamura, H. Kakinuma, H. Umemiya, H. Amada, N. Miyata, K. Taniguchi, K. Bando, M. Sato**.** *Bioorg. Med. Chem. Lett.* **2004**, *14*, 333.
49. X. Zhao, M. Xin, W. Huang, Y. Ren, Q. Jin, F. Tang, H. Jiang, Y. Wang, J. Yang, S. Mo, H. Xiang**.** *Bioorg. Med. Chem.* **2015**, *23*, 348.
50. M.A. Kashem, R.M. Nelson, J.D. Yingling, S.S. Pullen, A.S. Prokopowicz, III, J.W. Jones, J.P. Wolak, G.R. Rogers, M.M. Morelock, R.J. Snow, C.A. Homon, S. Jakes**.** *J. Biomol. Screening* **2007**, *12*, 70.

Graphical abstract

Synthesis and Biological Evaluation of Irreversible EGFR Tyrosine Kinase Inhibitors Containing Pyrido[3,4-*d*]pyrimidine Scaffold

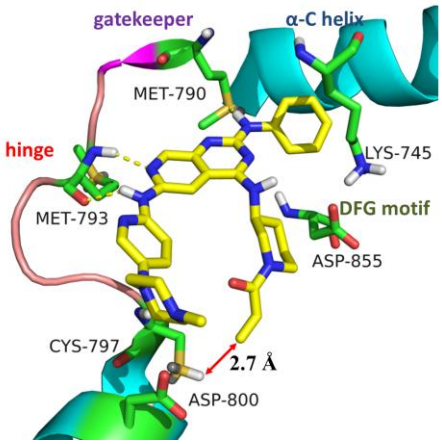

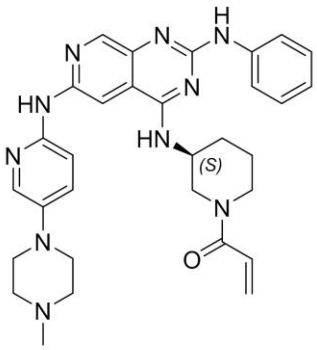

25h

	IC_{50}
$EGFR^{WT}$	1.9 nM
$EGFR^{L858R}$	1.7 nM
$EGFR^{L858R/T790M}$	23.3 nM
HCC827 cells	0.025 μM
H1975 cells	0.49 μM
A549 cells	0.99 μM

Highlights

►2,4,6-Trisubstitued pyrido[3,4-*d*]pyrimidine derivatives was designed as Irreversible EGFR-TKIs. ►Compound **25h** inhibited HCC827 and H1975 cells growth with the IC_{50} values of 0.025 μM and 0.49 μM, respectively. ►Compound **25h** displayed potent inhibitory activity against the $EGFR^{L858R}$ (IC_{50} = 1.7 nM) and $EGFR^{L858R/T790M}$ (IC_{50} = 23.3 nM). ►**25h** could remarkably inhibit cancer growth at the dose of 50 mg/kg in established nude mouse HCC827 xenograft model *in vivo*.